

***Compact Lightweight Power PEMFC Operating From  
a Unique Hydrogen Generating System***

Final Report

Robert Theriault

November 1995

Prepared for:

**U.S. ARMY RESEARCH OFFICE**  
P.O. Box 12211  
Research Triangle Park, NC 27709-2211

Contract No. DAAH04-93-C-0054

Prepared by:

**GINER, INC.**  
14 Spring Street  
Waltham, MA 02154-4497

19960209 108

APPROVED FOR PUBLIC RELEASE;

DISTRIBUTION UNLIMITED.

DTIC QUALITY INSPECTED 1

**THE VIEWS, OPINIONS, AND/OR FINDINGS CONTAINED IN THIS REPORT ARE  
THOSE OF THE AUTHOR(S) AND SHOULD NOT BE CONSTRUED AS AN  
OFFICIAL DEPARTMENT OF THE ARMY POSITION, POLICY, OR DECISION,  
UNLESS SO DESIGNATED BY OTHER DOCUMENTATION.**

## REPORT DOCUMENTATION PAGE

Form Approved  
OMB No. 0704-0188

Public reporting burden for this collection of information is estimated to average 1 hour per response, including the time for reviewing instructions, searching existing data sources, gathering and maintaining the data needed, and completing and reviewing the collection of information. Send comments regarding this burden estimate or any other aspect of this collection of information, including suggestions for reducing this burden, to Washington Headquarters Services, Directorate for Information Operations and Reports, 1215 Jefferson Davis Highway, Suite 1204, Arlington, VA 22202-4302 and to the Office of Management and Budget, Paperwork Reduction Project (0104-0188), Washington, DC 20503.

1. AGENCY USE ONLY (Leave blank)		2. REPORT DATE 19 Sep 95	3. REPORT TYPE AND DATES COVERED 10 Sep 93 - 09 Mar 95
4. TITLE AND SUBTITLE  Compact Lightweight Power PEMFC Operating From a Unique Hydrogen Generating System			5. FUNDING NUMBERS  DAAH04-93-C-0054
6. AUTHOR(S)  Robert Theriault			
7. PERFORMING ORGANIZATION NAME(S) AND ADDRESS(ES)  GINER, INC. 14 Spring Street Waltham, MA 02154-4497			8. PERFORMING ORGANIZATION REPORT NUMBER  C93-22 F
9. SPONSORING/MONITORING AGENCY NAME(S) AND ADDRESS(ES)  U.S. Army Research Office P.O. Box 12211 Research Triangle Park, NC 27709-2211			10. SPONSORING/MONITORING AGENCY REPORT NUMBER  ARO 32155. I-CH
11. SUPPLEMENTARY NOTES  The views, opinions and/or findings contained in this report are those of the author(s) and should not be construed as an official Department of the Army position, policy, or decision, unless so designated by other documentation.			
12a. DISTRIBUTION/AVAILABILITY STATEMENT  Approved for public release; distribution unlimited.		12b. DISTRIBUTION CODE	
13. ABSTRACT (Maximum 200 words)  <p>The goal of this program was to investigate the feasibility, for the military, of a 120-watt, 20,000-watt-power source weighing near ten pounds. An air-breathing proton-exchange membrane fuel cell (PEMFC) utilizing hydrogen from Lithium Borohydride (<math>\text{LiBH}_4</math>) could theoretically meet this specification. Giner, Inc. has established that a hydrogen generator, utilizing <math>\text{LiBH}_4</math>, provides a hydrogen current flux of 150 Amps/<math>\text{ft}^2</math> with about 60% long-term utilization. Additionally, Giner, Inc. demonstrated a 120-watt fuel cell system, which operated at approximately 12 volts at 100 Amps/<math>\text{ft}^2</math> (10 amps through a 0.1-<math>\text{ft}^2</math> active area). Integrating the two systems will require further effort and development work.</p>			
14. SUBJECT TERMS  proton-exchange membrane fuel cell, lithium borohydride, lightweight fuel cell			15. NUMBER OF PAGES  50
			16. PRICE CODE
17. SECURITY CLASSIFICATION OF REPORT  UNCLASSIFIED	18. SECURITY CLASSIFICATION OF THIS PAGE  UNCLASSIFIED	19. SECURITY CLASSIFICATION OF ABSTRACT  UNCLASSIFIED	20. LIMITATION OF ABSTRACT

## TABLE OF CONTENTS

REPORT DOCUMENTATION PAGE .....	ii
TABLE OF CONTENTS .....	iii
LIST OF TABLES AND FIGURES .....	iv
EXECUTIVE SUMMARY .....	1
1.0 PHASE I: HYDROGEN GENERATOR DEVELOPMENT .....	4
1.1 Summary .....	4
1.2 Introduction .....	4
1.3 Experimental .....	7
1.4 Results and Discussion .....	8
1.5 Conclusions and Recommendations .....	15
2.0 PHASE II: LIGHTWEIGHT PEMFC DEVELOPMENT .....	16
2.1 Summary .....	16
2.2 Introduction .....	16
2.3 Experimental .....	17
2.4 Results and Discussion .....	23
2.5 Conclusions and Recommendations .....	25
APPENDIX A. Permeability Calculation .....	A-1
APPENDIX B. Summary of System Designs .....	B-1

## LIST OF TABLES AND FIGURES

Table 1.	Physical and Economic Properties of LiBH <sub>4</sub> . . . . .	1
Table 2.	Characteristics of Hydrogen-Generating Fuels . . . . .	5
Table 3.	Change in Dew Point Conditions from the Saturator . . . . .	13
Figure 1.	Fuel Cell System with Titanium End Plates (18 lbs) . . . . .	3
Figure 2.	Fuel Cell System with Pneumatic End Plates (12 lbs) . . . . .	3
Figure 3.	Water Requirements for various Chemical Hydrides . . . . .	6
Figure 4.	Experimental Setup . . . . .	7
Figure 5.	Hydrogen Generator system Flowsheet . . . . .	8
Figure 6.	Performance of a Hydrogen Generator . . . . .	9
Figure 7.	Performance of a Hydrogen Generator . . . . .	9
Figure 8.	Effect of Dew Point on a 1.0-g LiBH <sub>4</sub> Reactor System . . . . .	10
Figure 9.	Characteristics of a Single-Membrane Giner Saturator Running on Dry Air Feed . . . . .	11
Figure 10.	Effect of Membrane Material on a 1.0-g LiBH <sub>4</sub> Reactor System . . . . .	11
Figure 11.	Effect of Pellet Density on a 1.0-g LiBH <sub>4</sub> Reactor System . . . . .	12
Figure 12.	Pellet Density vs. Pressure . . . . .	12
Figure 13.	Effect of Membrane Equilibration of a 1.0-g LiBH <sub>4</sub> Reactor System . . . . .	13
Figure 14.	Assembly Drawing (Top View) for System Design 13 (Baseline) . . . . .	17
Figure 15.	Titanium End Plate . . . . .	18
Figure 16.	Polysulfone Anode Frame . . . . .	19
Figure 17.	Hydrophilic Anode Collector . . . . .	20
Figure 18.	Cathode Collector . . . . .	21
Figure 19.	Titanium Supporting Gasket . . . . .	21
Figure 20.	Membrane and Electrode Assembly . . . . .	22
Figure 21.	Performance of H <sub>2</sub> /Air PEM Fuel Cell (9322-1715, 19-Cell Stack) . . . . .	23
Figure 22.	Performance of H <sub>2</sub> /Air PEM Fuel Cell (19-Cell Stack) . . . . .	24

## EXECUTIVE SUMMARY

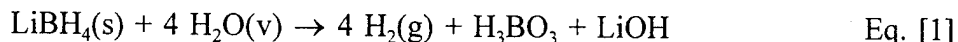
The goal of this program was to investigate the feasibility for the military of a 120-watt, 20,000-watt-power source weighing near 10 pounds. The power source should operate unattended and quietly for about two months. At present, no known devices, including motor generator sets and batteries, can meet these demanding specifications.

However, an air-breathing proton-exchange membrane fuel cell (PEMFC) utilizing hydrogen from Lithium Borohydride ( $\text{LiBH}_4$ ) could theoretically meet this specification. Properties of  $\text{LiBH}_4$  are summarized in **Table 1**. A typical mission of 65 days needs on average 300 Whrs/day, thus requiring approximately 20 kWhr of fuel. This 20 kWhr mission requires about 6 lbs. of  $\text{LiBH}_4$ , which has a capacity of 0.31 lbs. fuel/kWhr.

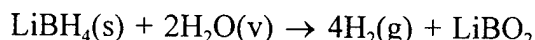
**Table 1. Physical and Economic Properties of  $\text{LiBH}_4$**

M.W. (g)	Moles $\text{H}_2(\text{g})$ Moles Fuel	Lbs Fuel/ kWhr	\$/lb 1992	Cost \$/kWhr
21.8	4.0	0.31	857	266

Lithium borohydride reacts with water as:

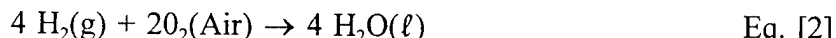


Another possible and preferential reaction path is



This reaction path requires less water to produce the equivalent amount of  $\text{H}_2$  since only 2 moles  $\text{H}_2\text{O}$  are required to produce the 4 moles  $\text{H}_2$  for the fuel cell reaction.

The hydrogen is then used in a PEMFC whose overall reaction (in the presence of platinum catalyst) is:



A fuel cell operating on air will evaporate essentially all of the product water at the upper end of the ambient temperature specification; about 125°F. If the fuel cell used all of the oxygen in the air stream, then the air exhaust could be directly contacted with the hydride. The hydride would react with the water vapor producing hydrogen and the hydrogen would be fed to the cells. Typically, however, for good performance, fuel cells require reaction air flow rates of two to three times theoretical. If such exhaust air were contacted with hydride, the excess oxygen would consume much of the generated hydrogen when it reached the fuel chambers of the cells. Also, the excess nitrogen would cause performance loss at the fuel cell anodes. Therefore, Giner, Inc. proposed that the product water be transferred from the air exhaust to the hydride through an

ionomer membrane, which would allow water vapor to pass, but not oxygen or nitrogen. An ionomer membrane is chosen because it has sufficient high water-vapor-transport behavior for the high water flow rates required. This report will examine the results of the hydrogen generator development process and the fuel cell stack development. For convenience, the development program that was conducted is divided into two phases; Phase I, HYDROGEN GENERATOR DEVELOPMENT and Phase II, LIGHTWEIGHT PEM FUEL CELL DEVELOPMENT.

In the Phase I studies, it was demonstrated that it is feasible to produce hydrogen from LiBH<sub>4</sub> utilizing Nafion 112 as a water-transport vehicle. A maximum hydrogen current flux of 150 Amps/ft<sup>2</sup> is possible; however, this was not sustainable over long periods of time. Additionally, it was possible to recover 58% of the theoretical level of hydrogen that should be produced with a one-gram sample of LiBH<sub>4</sub>. Further work is required to develop a hydrogen generator/hydride reactor that will sustain a 120-watt fuel cell system.

For the Phase II study, Giner, Inc. demonstrated the feasibility of a baseline lightweight, 19-cell PEMFC stack that operated with excess liquid water on the anode side and provided sufficient "proton-water pumping" to meet the heat management water evaporation requirements of the 120-watt stack. The approach of providing the cooling water was embodied in a hydrophilic current collector which contacted and supplied water to a specially designed anode catalyst. The development of this unique anode structure resulted in high electro-osmotic water transport from anode to cathode. The cooling water was transported in proportion to the local current and to the waste heat flux.

Other unique concepts demonstrated in the baseline 19-cell PEMFC stack configurations included the fabrication and use of 1) machined-molded graphite collectors (molded at Giner, Inc.) and 2) pneumatic end plates that reduced the weight of the stack from 18 to 12 lbs. The 120-watt stack configured with solid Ti and pneumatic Al end plates is shown in **Figures 1** and **2**, respectively. The performance of the baseline 19-cell stack with Ti end plates was approximately 12 V at 10 A (100 Amps/ft<sup>2</sup>) or 120 watts, when operated with bottled H<sub>2</sub> and ambient air supplied by a blower fan. A similar 19-cell stack with pneumatic end plates (**Figure 2**) and air flowing through the channels by convective flow operated at 13.7 V at 7 A (70 Amps/ft<sup>2</sup>), or 96 watts. A description of some of the alternative stack designs and tests that led to the development of the baseline PEMFC stacks is presented in the attached **APPENDIX B**.

The stack could only operate efficiently for short periods of time due to excess flooding of the gas flow fields from the circulating anode water feed. Also, humidification was not sufficient and there was local drying at gas inlets.

There was no integration of the hydride and PEMFC system because of the limited funding available in this initial program; however, it is projected the weight of the 100-watt PEMFC (12 lbs) with pneumatic end plates and the 20 kWhr of LiBH<sub>4</sub> fuel (6 lbs) when integrated into a breadboard system would be approximately 20 lbs. With advanced development (i.e., thinner air cathode plates and higher performance membranes) the weight could be reduced to 10 to 15 lbs.

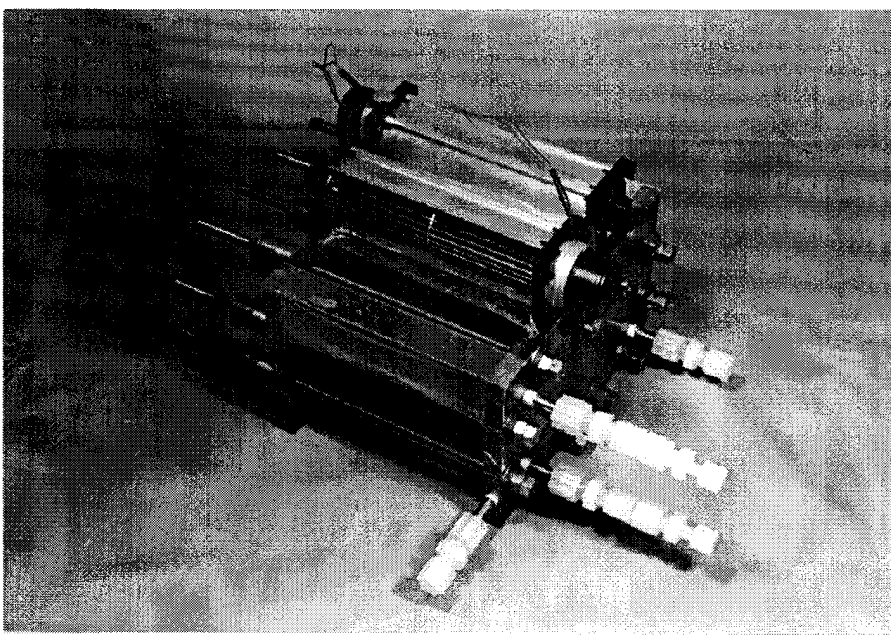


**Figure 1. Fuel Cell System with Titanium End Plates (18 lbs)**

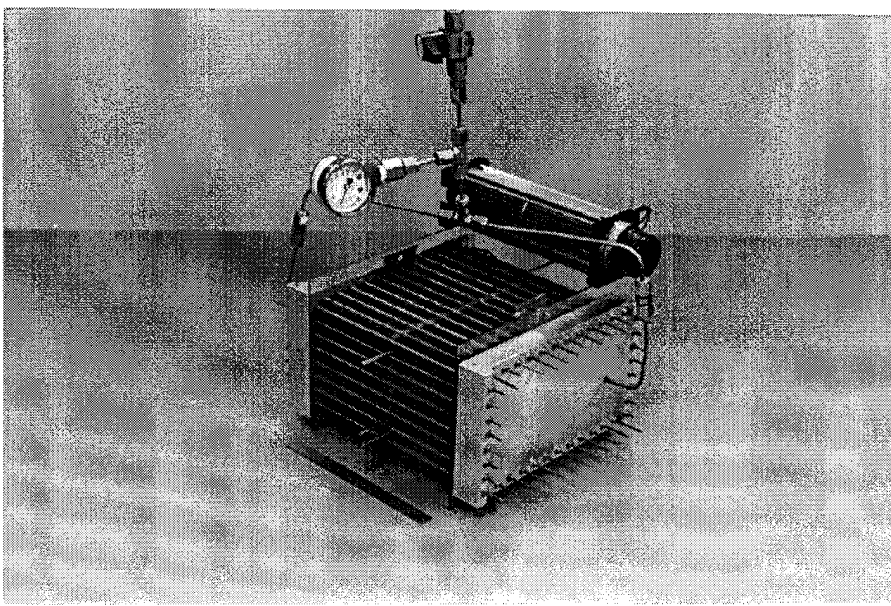


**Figure 2. Fuel Cell System with Pneumatic End Plates (12 lbs)**

## 1.0 PHASE I: HYDROGEN GENERATOR DEVELOPMENT

### 1.1 Summary

The purpose of this Phase I study was to determine the feasibility of developing a portable hydrogen generator system based on the reactions of water vapor with LiBH<sub>4</sub>. The novel concept investigated was the use of an ionomer membrane (Nafion® 112) to selectively transport water vapor from humidified air to the LiBH<sub>4</sub> reactant. All experiments conducted at Giner, Inc. utilized one-gram samples of LiBH<sub>4</sub>. The LiBH<sub>4</sub> was prepared by pressing it into a circular pellet with a one-inch diameter and an 1/8" height. The LiBH<sub>4</sub> pellet was placed on top of a Nafion 112 membrane, which was anchored inside the hydride reactor. Humidified air (5000 sccm) was dispersed across the other side of the Nafion 112 membrane, which then selectively transported water vapor to the LiBH<sub>4</sub> pellet.

We were able to produce hydrogen from LiBH<sub>4</sub> utilizing Nafion 112 as a water-transport vehicle. A maximum hydrogen current flux of 150 Amps/ft<sup>2</sup> is possible; however, this was not sustainable over long periods of time. Additionally, we were able to recover 58% of the theoretical level of hydrogen that should be produced with a one-gram sample of LiBH<sub>4</sub>. Further work is required to develop a hydrogen generator/hydride reactor that will sustain a 120-watt fuel cell system.

### 1.2 Introduction

**Choice of Chemical Hydride:** Lithium borohydride, because it provides superior system weight, was chosen as the fuel for the chemical hydride system. This is indicated in **Table 2** which lists the characteristics of several fuels. The excess cost for LiBH<sub>4</sub> is expected to significantly decrease with increasing production demands.

Secondly, overall system weight and volume depend significantly on the amount of water required by the fuel. This affects the size and power consumption of the condenser on the fuel cell air-exhaust, where the product water is captured. Of course, the need to carry extra water with the system increases size and weight. **Figure 3** shows the chemical stoichiometry for selected metals and hydrides. **Figure 3A** describes such chemistry for metals which are used to form hydrogen from water. The fuel cell is shown as using all of the hydrogen from the generator, and producing water, which is valuable because it can be re-used in the metal/hydrogen reaction. However, in this case, the fuel cell product water accounts at most for only half of the water needed by the metal, the remainder having to be carried with the system. The system size and weight suffer from the extra weight of water as well as the tankage to hold the extra water.

**Figure 3B** describes a class of hydrides having a single metal ion, examples being LiH and CaH<sub>2</sub>. They require an amount of water equal to that produced by the fuel cell. It would seem that these hydrides have an ideal water balance with the fuel cell. In reality, they are still somewhat deficient, because some of the product water leaves the system in the exhaust reaction air of the fuel cell. In order to reclaim all of the fuel cell water on a dry day, the temperature of the air used to cool the condenser would typically have to be at a lower temperature than the air used to feed the fuel cell. Clearly, this is impractical for the application being considered here. Some water will no doubt have to be carried in such systems.

**Figure 3C** describes the metal-borohydrides, such as  $\text{LiBH}_4$  and  $\text{NaBH}_4$ , composed of two metal ions, one of which is boron (or aluminum). These require only half the water made by the fuel cell, due to the formation of borate as a reaction product. Of course, the equipment needed to reclaim smaller fractions of the water will be exponentially smaller, given the exponential nature of heat transfer processes.

Therefore, since this application is driven largely by weight and volume, the technically superior lithium borohydride was chosen to be used in the chemical hydride system.

**Table 2. Characteristics of Hydrogen-Generating Fuels**

Fuel	M.W. (g)	Mole H <sub>2</sub> / Moles Fuel	Lbs Fuel/ kWhr	\$/Lb 1992	Cost \$/kWhr
$\text{LiBH}_4$	21.8	4.0	0.31	857	266
LiH	8.0	1.0	0.46	61	28
$\text{NaBH}_4$	37.83	4.0	0.54	34	18
$\text{LiAlH}_4$	37.95	4.0	0.55	89	49
$\text{MgH}_2$	26.33	2.0	0.76	81	62
$\text{NaAlH}_4$	54.00	4.0	0.78	70	55
$\text{CaH}_2$	41.08	2.0	1.18	24	28
Al	26.98	1.5	1.03	6-7	7
Mg	24.32	1.0	1.39	12	17
$\text{CH}_3\text{OH}$	32	3.0	0.6	1.10	0.7
$\text{H}_2^{\text{a}}$	2	1.0	12	13	156
$\text{H}_2^{\text{b}}$	2	1.0	1.2	13	16
Diesel fuel <sup>c</sup>			0.45	0.14	0.06

a) in commercial pressurized cylinders

b) absorbed on carbon (cryogenic)

c) 10 gallons in a tank @ 50% HHV

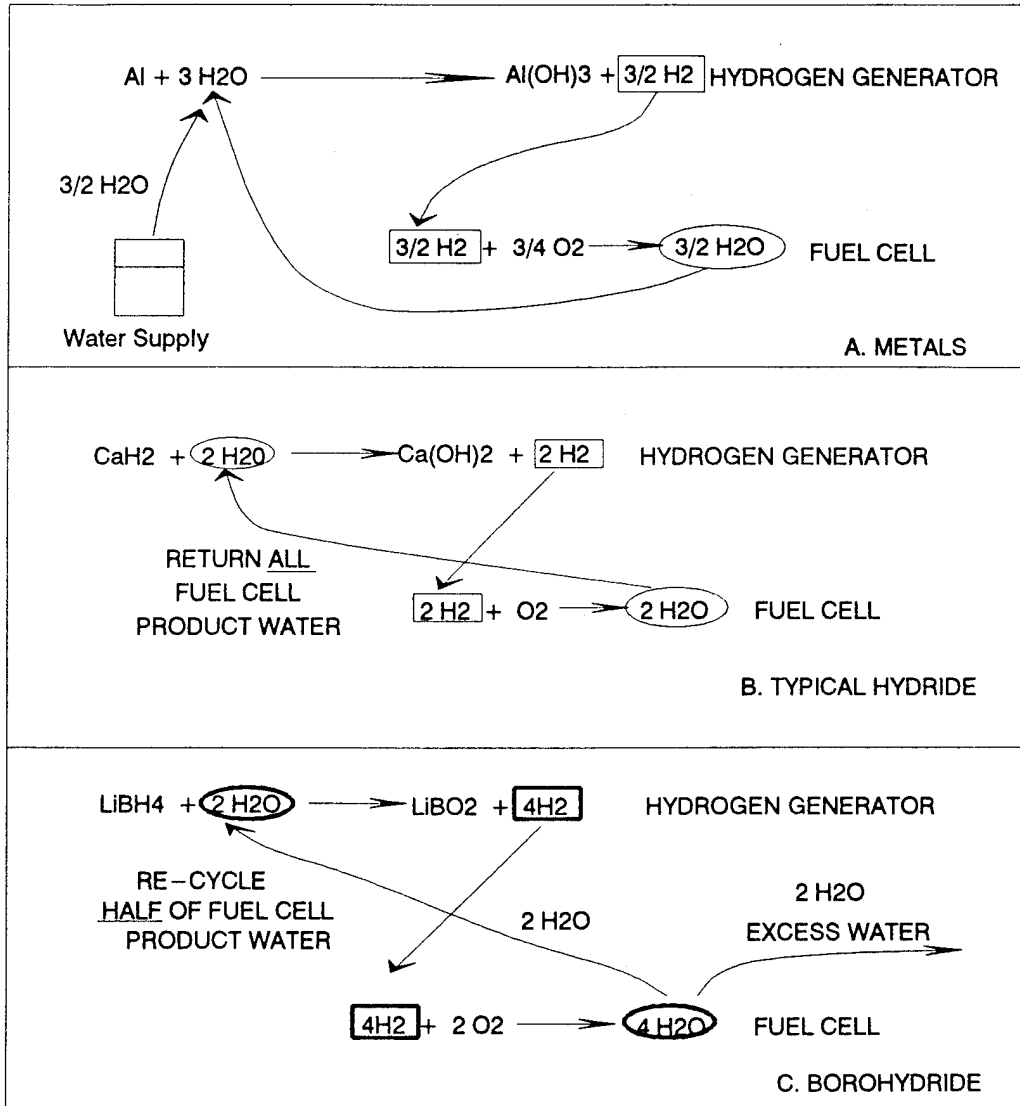


Figure 3. Water Requirements for various Chemical Hydrides

### 1.3 Experimental

**Phase I Procedure:** The experimental hydrogen generator system consists of a single-cell membrane saturator, a hydride sample holder, and a hydrogen gas measuring device (see **Figure 4**). Humid air was generated by passing dry air by a Nafion 120 membrane inside the saturator, with 6.25 in<sup>2</sup> of active area. Water vapor transported through the Nafion 120 from liquid water, which communicated with the Nafion 120 membrane. The liquid water pressure into the saturator was controlled by maintaining a constant back pressure, P<sub>1</sub>, of approximately 13" of water. Air flow (bottled air, U.S.P. Medical Airco) to the saturator was controlled with a flow-tube flowmeter (Omega 0-7500 sccm air). System temperatures were controlled by temperature controllers, (Omega, CN9000A), thermocouples (type K), and heating pads. Temperatures were maintained so as to assure water vapor was contacting the Nafion 112 membrane. The Nafion 112 had an active area of 0.75 in<sup>2</sup>. Hydrogen gas produced in the LiBH<sub>4</sub> (Alfa Aesar, Stock #32563) sample holder was measured by timing the displacement of a water column between V<sub>1</sub> and V<sub>2</sub>.

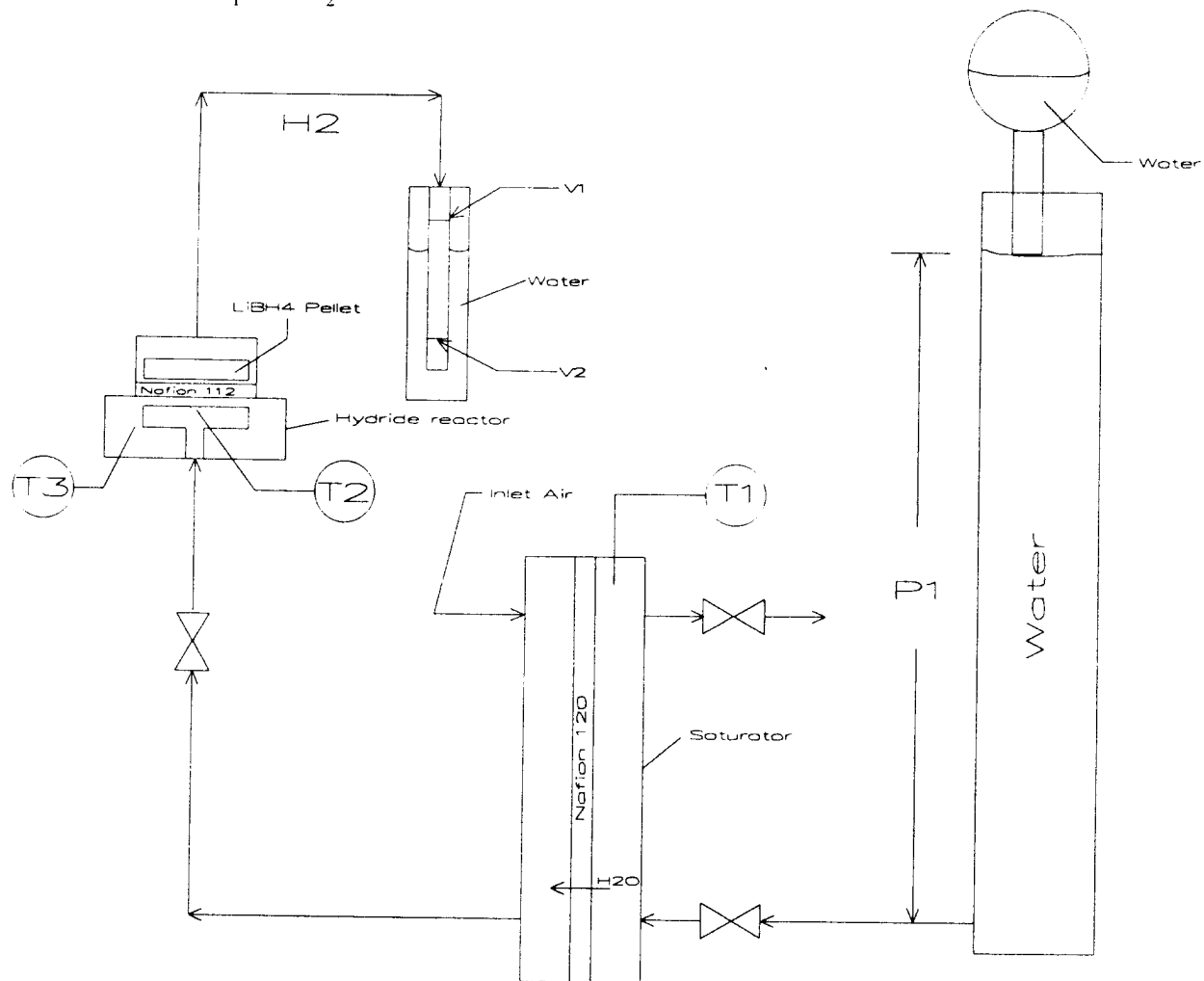
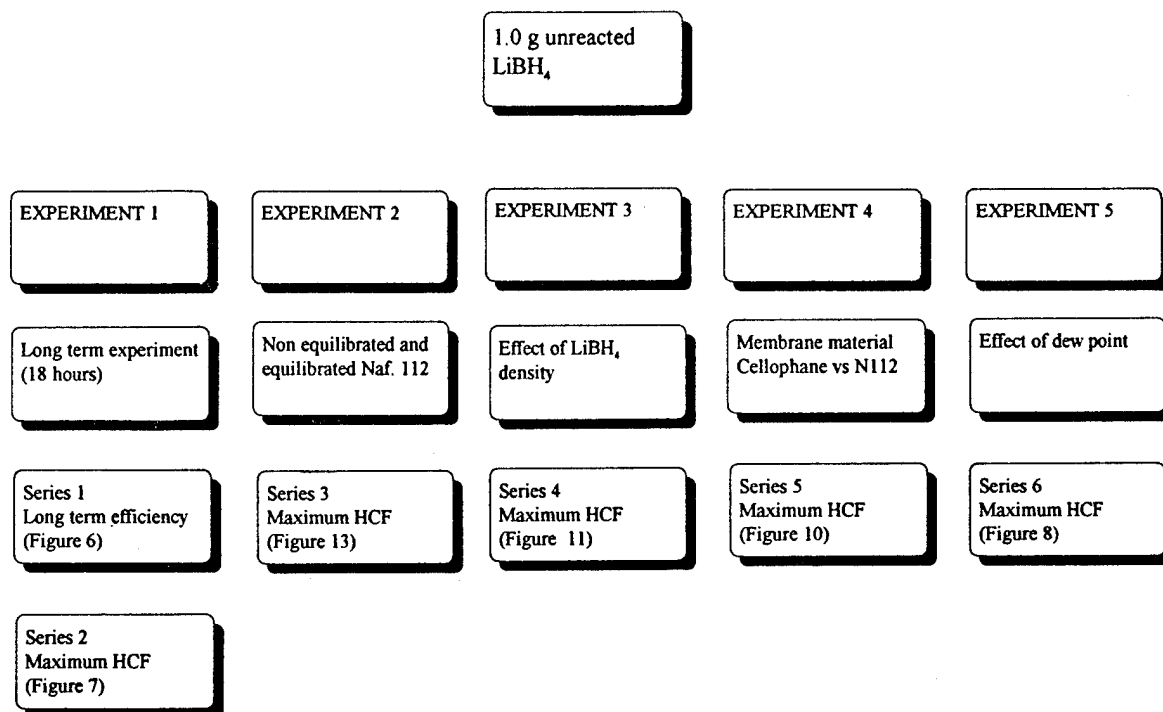


Figure 4. Experimental Setup

COPY AVAILABLE TO DTIC DOES NOT PERMIT FULLY LEGIBLE REPRODUCTION

Various experiments were completed with the hydrogen generator system. The experimental design and hydrogen generation system flow sheet is shown in **Figure 5**. All experiments used one gram of Lithium borohydride. Investigations included long-term operating effects, membrane effects, LiBH<sub>4</sub> bulk density effects, and dew point effects. Long-term operating effects were investigated to determine the total hydrogen production obtained from one gram of Lithium borohydride. Membrane effects included physical characteristics (non-equilibrated vs. equilibrated) and material (Nafion 112 vs. cellophane). Bulk density effects were investigated to show the relationship between pellet density and maximum hydrogen current flux (HCF). Additionally, the water vapor permeability of Nafion 112 was determined.



**Figure 5. Hydrogen Generator system Flowsheet**

#### 1.4 Results and Discussion

Hydrogen was successfully generated using the hydrogen generator system. The long-term efficiency and maximum hydrogen current flux was determined. **Figure 6** and **Figure 7** graphically present the results. Figure 6 shows that initially the efficiency is at theoretical levels, but after one hour begins to level off. Theoretically 1.0 g of LiBH<sub>4</sub> will produce 4 liters of hydrogen in just under 13 hours. Our system generated 2.30 liters of hydrogen in 18 hours. Our total utilization would be 58% based on the total hydrogen produced in the system. Figure 7 shows that the maximum hydrogen current flux was 150 Amps/ft<sup>2</sup> initially, but the current flux trended downward throughout the experiment until the system no longer produced hydrogen.

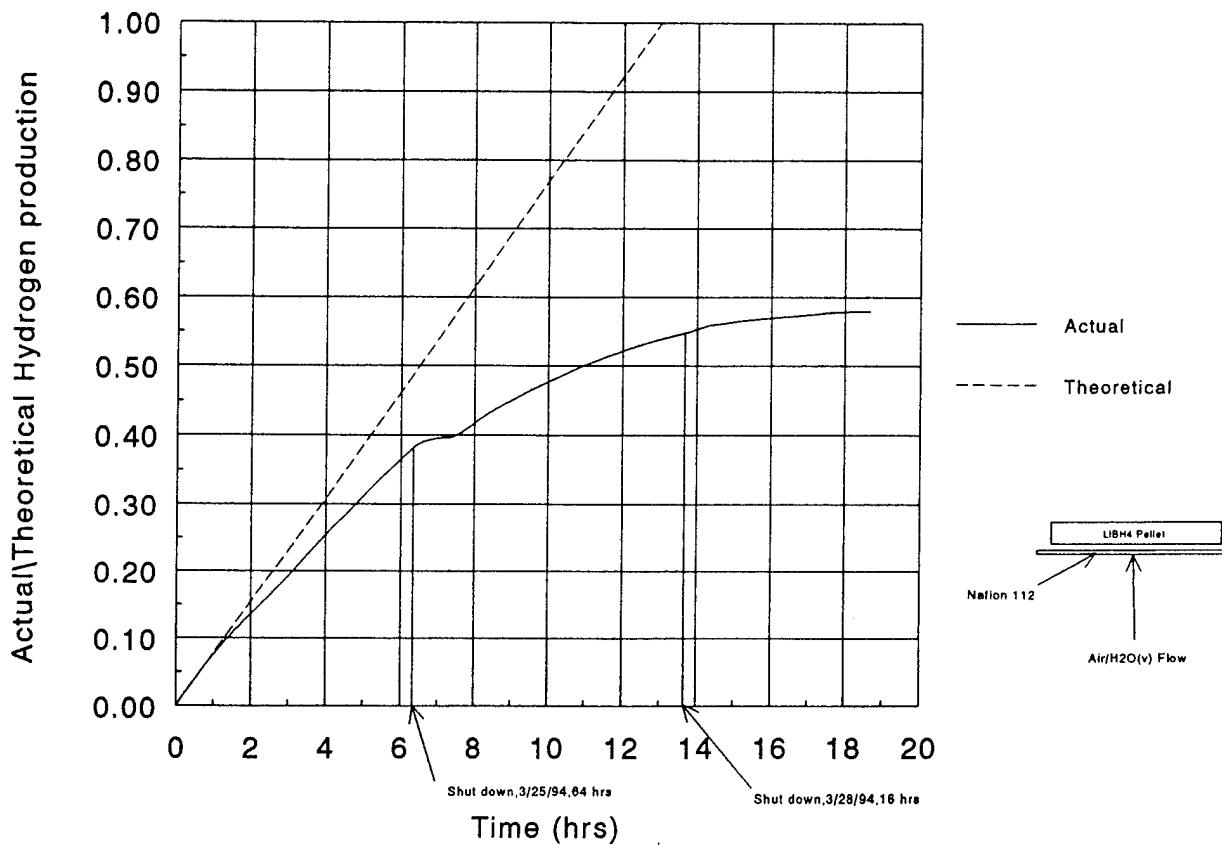


**Figure 6. Performance of a Hydrogen Generator**

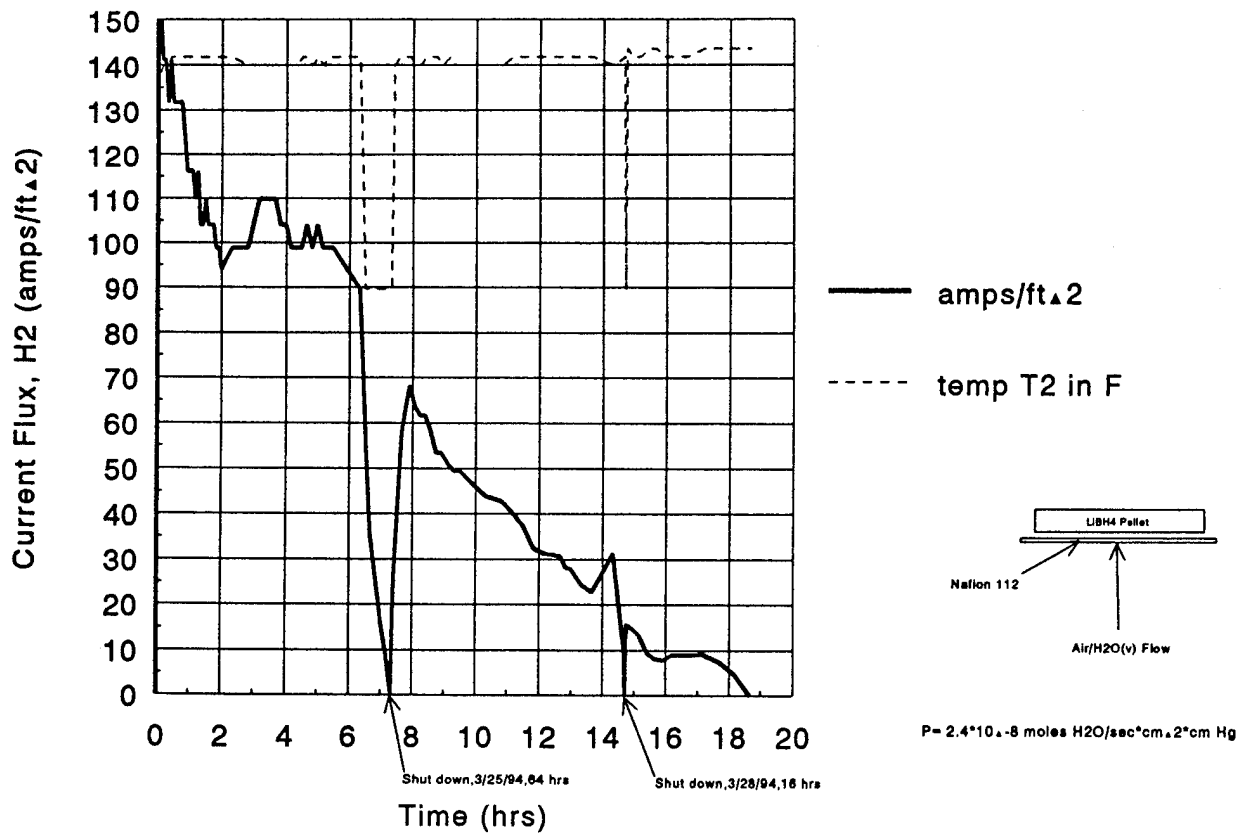


**Figure 7. Performance of a Hydrogen Generator**

The dew point entering the hydride sample showed an effect on the hydrogen current flux (HCF). **Figure 8** show initially that the higher the dew point the higher the corresponding hydrogen current flux. Note that the data on Figure 8 was obtained at an air flow rate of 5000 sccm. The HCF at a dew point of 84°F was about 30 Amps/ft<sup>2</sup> throughout the experiment. A dew point of 96°F initially gave a HCF of 124 Amps/ft<sup>2</sup>, subsequently rising to 140 Amps/ft<sup>2</sup>, and then falling below 120 Amps/ft<sup>2</sup>. A temperature of 140°F, which only raised the dew point to 104°F, started at 150 Amps/ft<sup>2</sup>, but continuously decreased to a point below 90 Amps/ft<sup>2</sup>. Differences also existed in the physical characteristics of each LiBH<sub>4</sub> pellet at each dew point test. Liquified byproducts surrounded the LiBH<sub>4</sub> pellet at a dew point of 84°F. The byproducts present at the bottom of the LiBH<sub>4</sub> pellet took on a dry foam-like texture at a dew point of 96°F. The byproducts, again present at the bottom of the pellet, became solid at a dew point of 104°F.

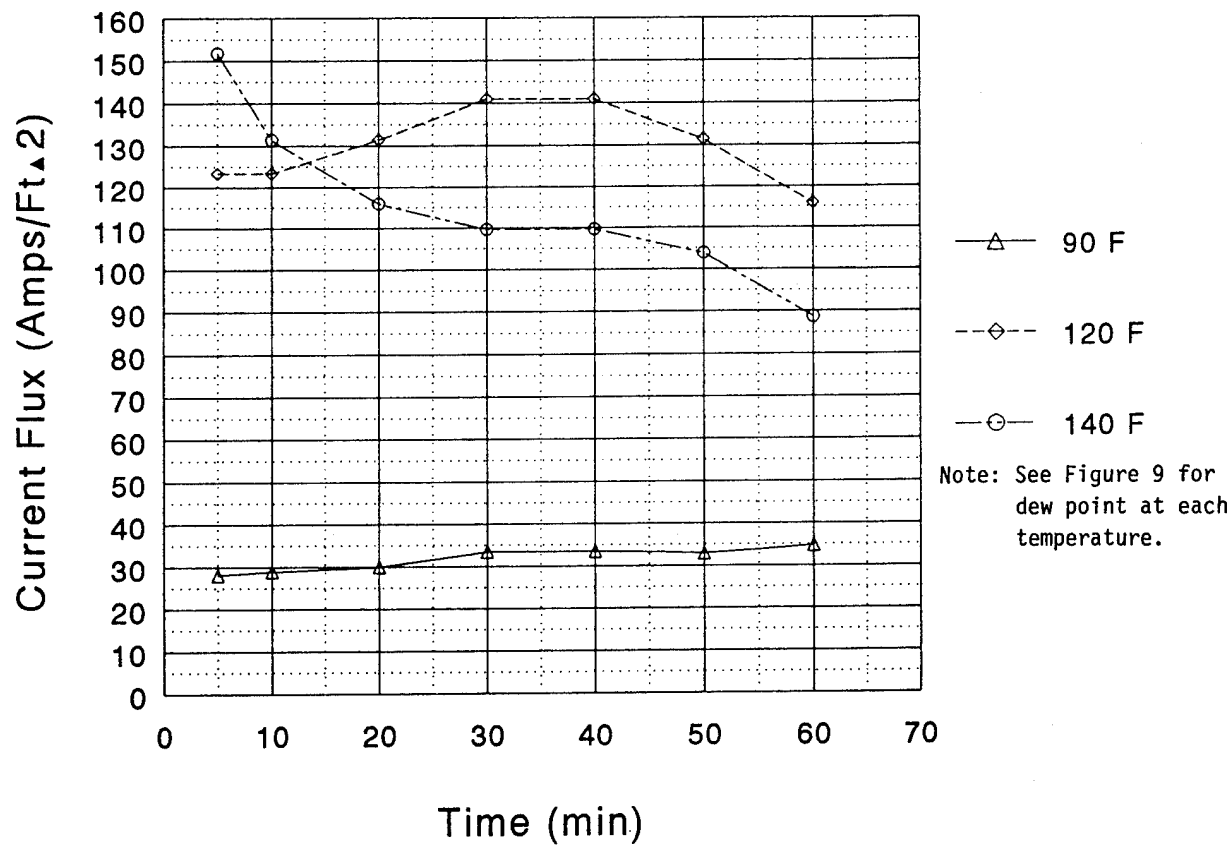


**Figure 8. Effect of Dew Point on a 1.0-g LiBH<sub>4</sub> Reactor System**

**Figures 10, 11, and 12** show the relationships between HCF and membrane material, pellet density, and (non) equilibrated membrane. Nafion 112 is clearly superior to cellophane as a water vapor transport membrane (See Figure 10). Cellophane initially gave a higher HCF than Nafion 112 (94 Amps/ft<sup>2</sup> vs. 76 Amps/ft<sup>2</sup>), but it quickly fell to 12 Amps/ft<sup>2</sup>, while Nafion 112 only fell to 52 Amps/ft<sup>2</sup>. Figure 11 shows that initially the higher the pellet density the higher the HCF, though this was not the situation at the end of the experiment. The line representing a pellet density of 0.57 g/cc crossed the line representing 0.46 g/cc at 35 minutes into the experiment. The highest pellet density did not finish the experiment with the highest HCF, though it

was still higher than unpelletized powder (density = 0.35 g/cc) in all cases. The HCF at all densities decreased steadily throughout the experiment. **Figure 13** shows that an unequilibrated Nafion 112 gave a higher HCF than equilibrated Nafion 112 at all points.

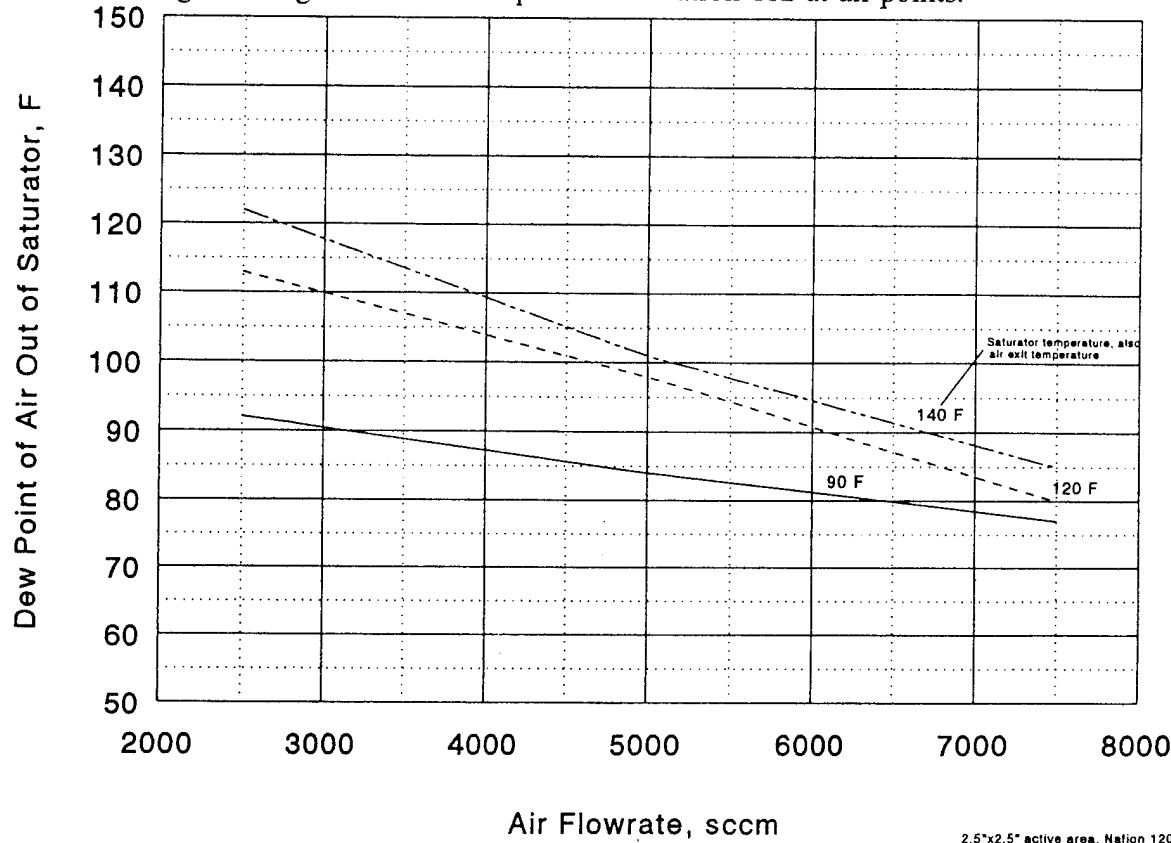


**Figure 9. Characteristics of a Single-Membrane Giner Saturator Running on Dry Air Feed**

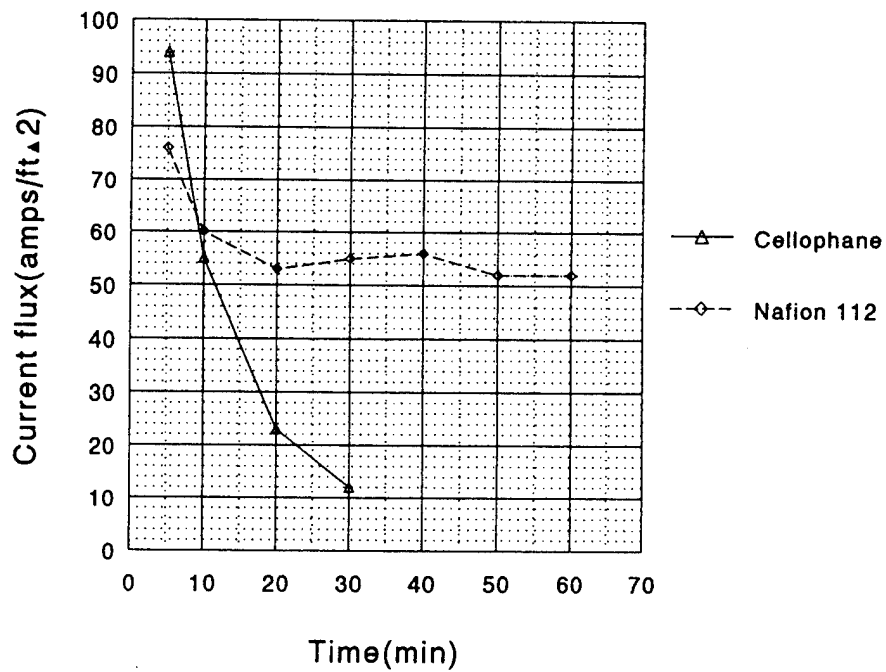


**Figure 10. Effect of Membrane Material on a 1.0-g LiBH<sub>4</sub> Reactor System**

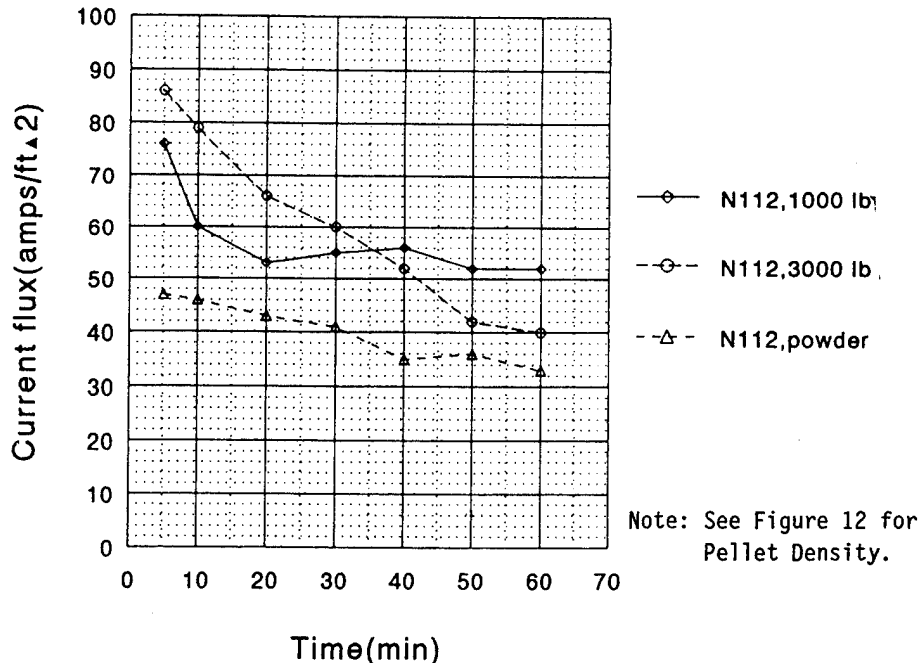


**Figure 11. Effect of Pellet Density on a 1.0-g LiBH<sub>4</sub> Reactor System**

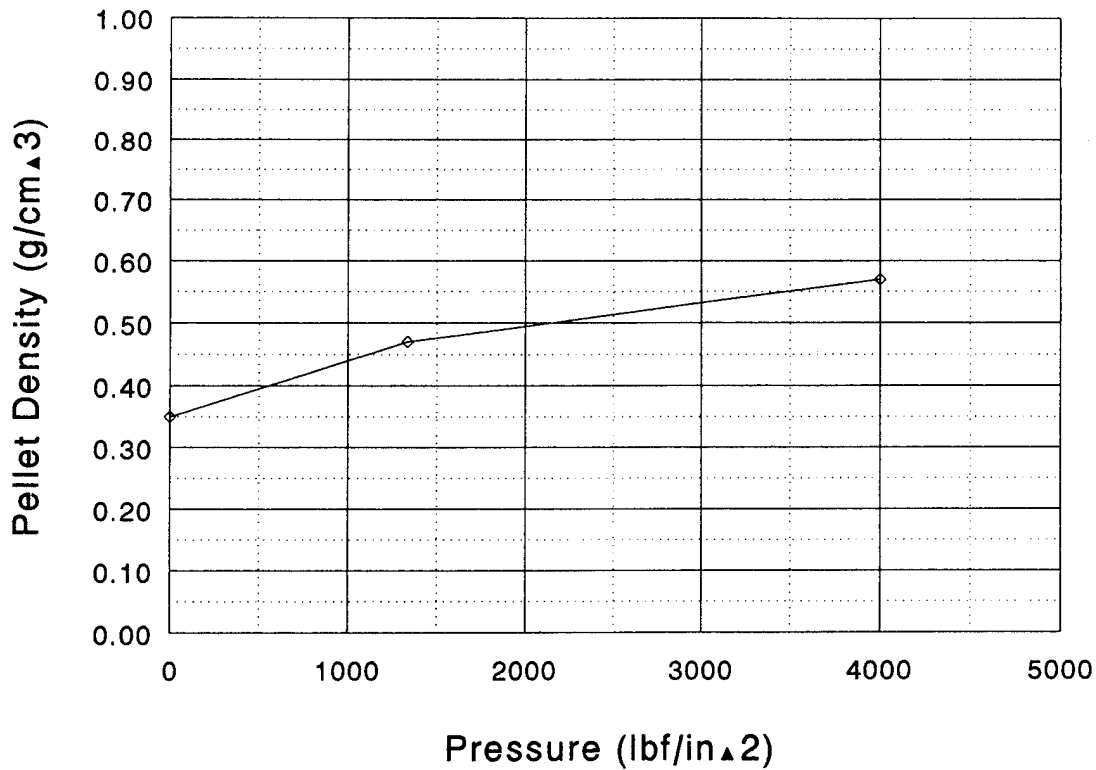


**Figure 12. Pellet Density vs. Pressure**

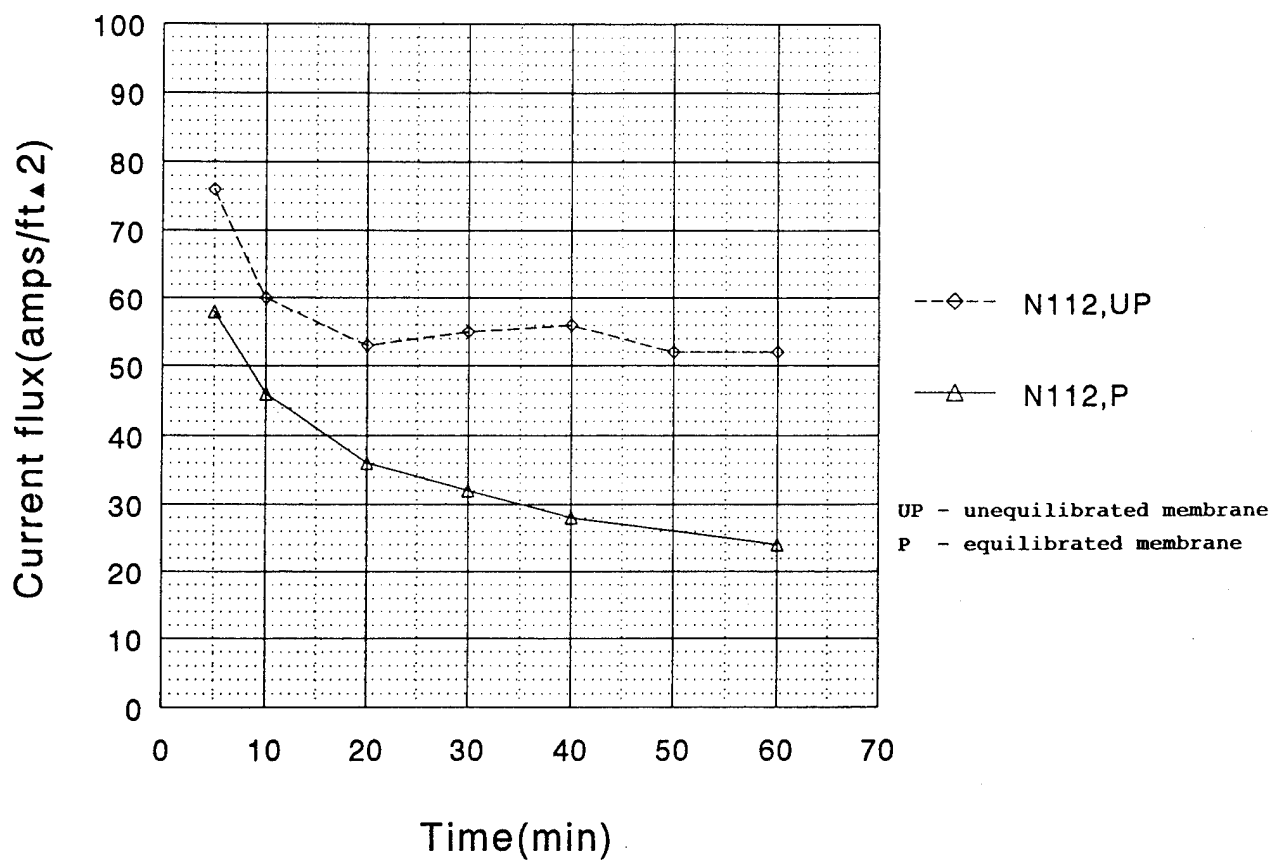


**Figure 13. Effect of Membrane Equilibration of a 1.0-g LiBH<sub>4</sub> Reactor System**

It should also be noted that a change in the air conditions from the saturator was noted while these data were accumulated. See **Table 3** for a chronological presentation of these observed changes.

**Table 3. Change in Dew Point Conditions from the Saturator**

Series	Figure Numbers	Dew Point Before	Dew Point After
1	6	101°F	No Data
2	7	No Data	No Data
3	13	No Data	No Data
4	11	No Data	No Data
5	10	No Data	81°F,
6	8	100°F (Replaced Nafion 120 in Saturator)	97°F

Figures 10 and 11 should be considered in relative terms instead of absolute terms. Nafion 112 is better than cellophane for example. Unfortunately the changing dew points were not observed immediately. Figure 8 confirms Figures 6 and 7 in that the maximum HCF obtained is about 150 Amps/ft<sup>2</sup>. Also this value steadily decreases over time. This HCF yielded a Nafion 112 permeability of about  $8.19 \times 10^{-6}$  cc H<sub>2</sub>O·cm/sec·cm<sup>2</sup>·cm Hg (see Appendix A).

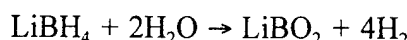
The two most important results obtained thus far are that a maximum HCF of 150 Amps/ft<sup>2</sup> is possible and that 58% of the LiBH<sub>4</sub> will be utilized in long-term usage. The maximum HCF also steadily declines over time to a value of zero based on our experimental system.

The lithium borohydride undergoes physical changes during reaction with water vapor. The hydride will flow in some cases like water. Eventually, the hydride will become encapsulated in "borate" shells, thus slowing down hydrogen production and eventually halting production even though unreacted LiBH<sub>4</sub> is still available. This factor appears to be the primary cause of the decreasing HCF over time. The decreasing dew point would also contribute to the problem, but the data would show that a 3% drop in dew point (Table 3, Series 6) results in a 30%-40% drop in HCF (Figure 8, 140°F). This does not make intuitive sense. The relationship between dew point and HCF should be linear according to the equation:

$$WDF = \frac{(P^*)(\Delta P)}{L}$$

where WDF = Water diffusional flux, P\* = Permeability, ΔP = Pressure difference across membrane and L = Membrane thickness.

The dew point would be represented by ΔP, which is a linear term in this equation. The water through the membrane is related to hydrogen production by a factor of 2 according to:



Each mole of water vapor will produce 2 moles of hydrogen. A 3% drop in dew point only accounts for a 6% drop in HCF. The remaining portion is attributable to the LiBO<sub>2</sub> forming around the LiBH<sub>4</sub>. Long-term data shows that HCF continues to decrease. This makes sense because the LiBO<sub>2</sub> is continuously produced throughout the length of the experiment.

The final fuel cell system will require  $1.04 \times 10^{-3}$  moles of hydrogen per second. A HCF of 2000 Amps/ft<sup>2</sup> would be required if one membrane with an active area of 0.1 ft<sup>2</sup> was used. The experimental HCF requires 14 Nafion 112 membranes with 0.1 ft<sup>2</sup> of active area. This also assumes that the maximum HCF of 150 Amps/ft<sup>2</sup> is maintained throughout the lifetime of the system.

## **1.5 Conclusions and Recommendations**

We are able to conclude that hydrogen can be produced from LiBH<sub>4</sub> in a system using Nafion 112 as a water vapor transport vehicle. Initially, the system provides a HCF of 150 Amps/ft<sup>2</sup>. However, limitations exist in this technique. Formation of "borates" over the long term are the most significant obstacle at this point. This factor causes the HCF to drop to zero in the long term. Further work is required to develop a hydrogen generator/hydride reactor that will sustain a 120-watt fuel cell system. The following problem requires further attention.

- (1) Conduct studies to determine the mechanism and kinetics of the LiBH<sub>4</sub> reaction with water and identify reaction products over time.
- (2) Investigate and develop a technique to manage "borates" from the hydrogen generator system as they are formed.
- (3) Investigate packaging techniques to achieve maximum utilization of LiBH<sub>4</sub>.

## **2.0 PHASE II: LIGHTWEIGHT PEMFC DEVELOPMENT**

### **2.1 Summary**

There is a need in the military for a 120-watt, 20,000-watt-hr power source weighing near ten pounds which can operate unattended and quietly for about two months. At present, no known devices can meet these specifications. Motor Generator sets are too large and too noisy. The best batteries available would weigh in the hundreds of pounds.

On the other hand, an air-breathing proton-exchange membrane fuel cell (PEMFC) integrated with a LiBH<sub>4</sub> reactor system, as described in Phase I of this report, could meet this specification.

Giner, Inc. developed a PEMFC that followed a bipolar series stack concept. The design utilized 19 membrane and electrode assemblies (MEA) with a 0.1 ft<sup>2</sup> active area. The baseline fuel cell stack was held in compression with titanium end plates. This fuel cell stack weighed 18 lbs. Substitution of lightweight pneumatic Al end plates for the Ti reduced the stack weight to 12 lbs. The Ti end plate stack delivered 11.7 volts and 117 watts at 10 A, 100 Amps/ft<sup>2</sup> (ASF) with bottled H<sub>2</sub> and air from a blower. A similar 19-cell stack with pneumatic end plates and air flowing through the channels by convective flow operated at 13.7 V and 96 watts at 7 A (70 ASF). Unfortunately, the fuel cell stacks were not adequate for long endurance due to simultaneous local drying and flooding of individual fuel cell compartments. The Phase II section of this report will describe the fuel cell system along with the test results obtained thus far. The present development challenges will also be addressed in this Phase II report.

### **2.2 Introduction**

The military is in need of electric power supplies which have high energy density, can be carried comfortably by the soldier, and can operate for long periods of time before discard or recharging. Traditional batteries, even the best ones available, cannot simultaneously provide long duration and high power at weights low enough for a person to carry. It is necessary to achieve an order of magnitude improvement in order to meet the missions of the military on the battlefield.

Fuel cells can easily provide the power levels required. The PEMFC is receiving much interest because of its ability to start and operate at low temperatures, because of its low weight, and because it contains no hazardous materials. When combined with suitable hydrogen generators, it promises to provide man-packed systems which operate for many hours at power levels sufficient to operate modern equipment.

Air-breathing PEMFC have been investigated in the past; however, they typically require external humidification and bipolar intercell cooling plates for sustained operation. Giner, Inc.'s approach was to investigate a possible simpler approach to water and thermal management. In the Giner, Inc. proposed concept, excess water was recirculated through the bottom of the anode chamber and was wicked up through use of a hydrophilic current collector to an anode catalyst structure. The water would help humidify the incoming gas. Also, some of the recirculated liquid water would be electrochemically transported from the fuel side of the membrane to the waste-heat-producing air-side, where the temperature would be automatically modulated by the evaporation of the water into the air stream.

## 2.3 Experimental

Giner, Inc. tested fifteen various fuel cell system configurations. The fuel cell system, designated System Design 13 (baseline), gave the best overall performance. The baseline is a 19-cell stack held in compression by titanium end plates. A brief description of some of the alternative stack designs and tests that led to the development of the baseline stack is presented in the attached **Appendix B**. **Figure 14** shows an assembly drawing of the baseline stack. Two identical cell units are illustrated to demonstrate that each cell cathode contacted the next cell anode. Figure 14 is not a scaled drawing. For example, the Teflon sealing gaskets (Part #7) are much thinner with respect to the other components in the stack. The corresponding drawing numbers and drawings can be used to obtain specific information about an individual part.

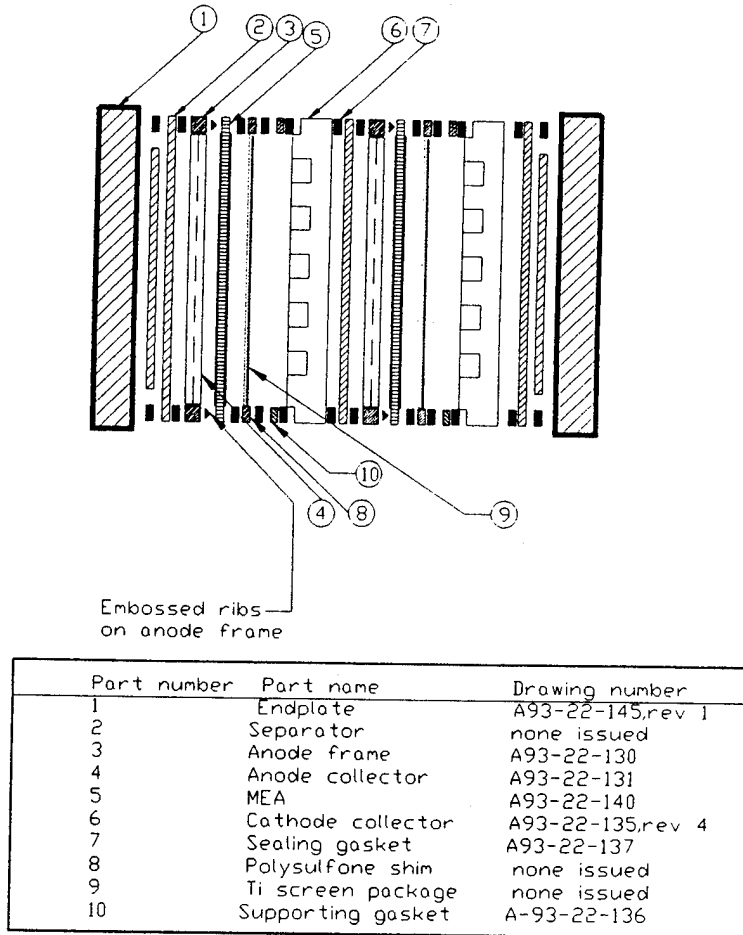


**Figure 14. Assembly Drawing (Top View) for System Design 13 (Baseline)**

In addition to titanium end plates, the baseline stack incorporated the following sub-assemblies: an anode compartment, a cathode compartment, a membrane and electrode assembly (MEA), and bipolar plates. Five-mil Teflon seals were used to seal port holes in each sub-assembly part.

The sub-assemblies were held together by torquing 12 5/16-24 S.S. nut and bolt joints, which then applied a compression force to the titanium end plates (see **Figure 15**) and the subassemblies. Figure 15 shows one end plate. The second end plate is the same, except the four most interior holes are missing from the end plate.

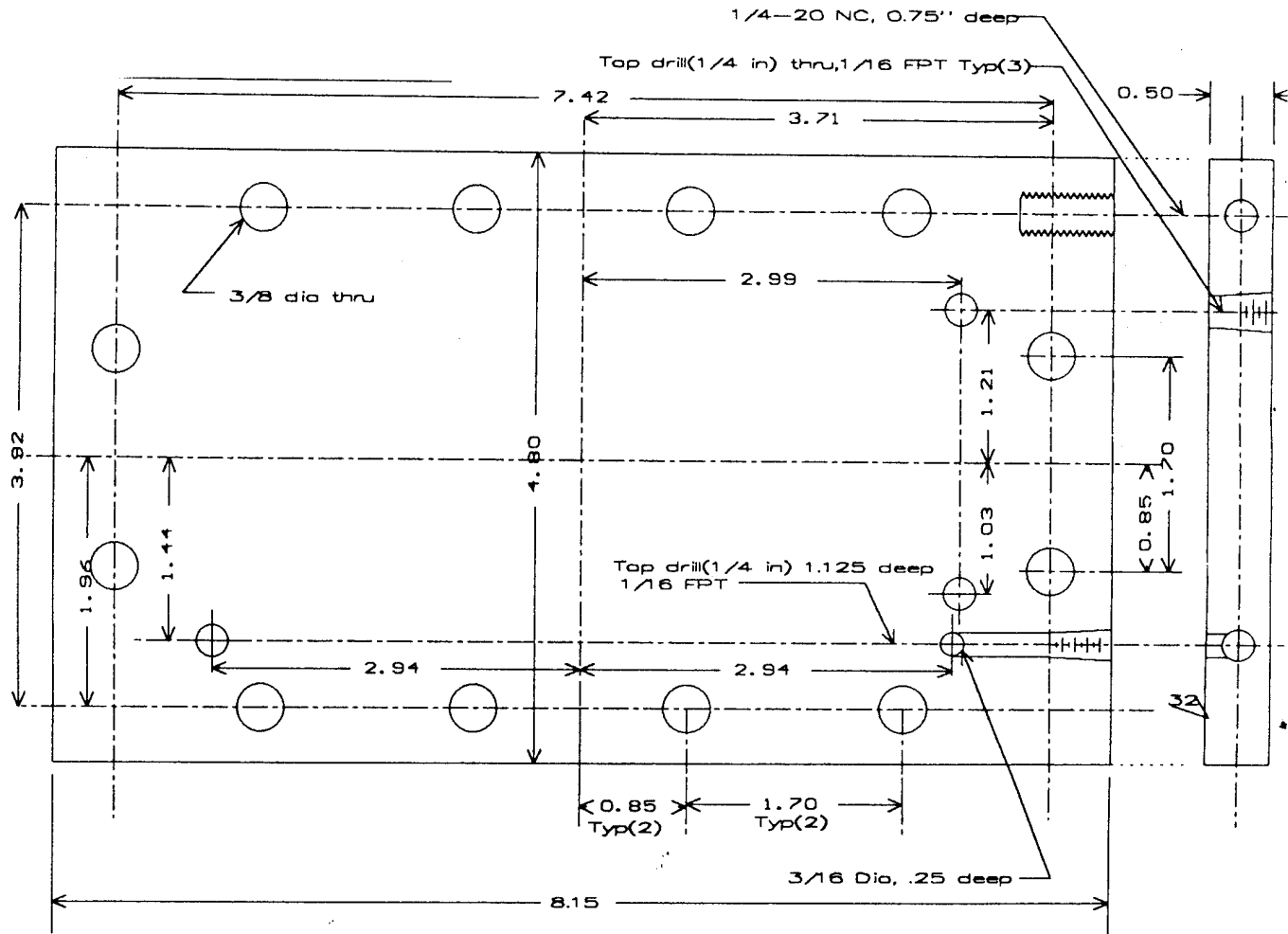


**Figure 15. Titanium End Plate**

Hydrogen and liquid water enter the fuel cell system from one end plate and flow toward the other end plate. Hydrogen enters at the upper right-hand side of the first end plate (Note that Figure 15 shows the interior face of the end plate, therefore the second end plate will project out from the paper surface) where it then flows through a manifold toward the second end plate. The hydrogen, while in the hydrogen inlet manifold, can only access the anode compartments of the fuel cell system. After flowing through a right-to-left labyrinth (see anode compartment description for details) in the anode compartment the hydrogen exits the anode at the lower right-hand corner of the anode compartment. The hydrogen then flows into the hydrogen exit manifold, which leaves the fuel cell system at the lower right-hand corner of the first end plate. Liquid water is introduced in the lower left-hand corner of the first end plate just below the level of the hydrogen exit stream. The water flows in a manifold toward the other end plate. The water enters each anode compartment just below the level of the hydrogen exit stream. The water

flows horizontally across the anode compartment toward the lower right-hand corner of the anode compartment. The water exits the anode compartment just below the level of the exiting hydrogen stream. Upon exiting the anode compartment, the water flows into an exit manifold, which exits the fuel cell system at the lower right-hand corner of the first end plate.

The anode compartment included two separate pieces. The first piece was a polysulfone anode frame (see **Figure 16**) with embossed sealing ribs on the MEA side of the frame.

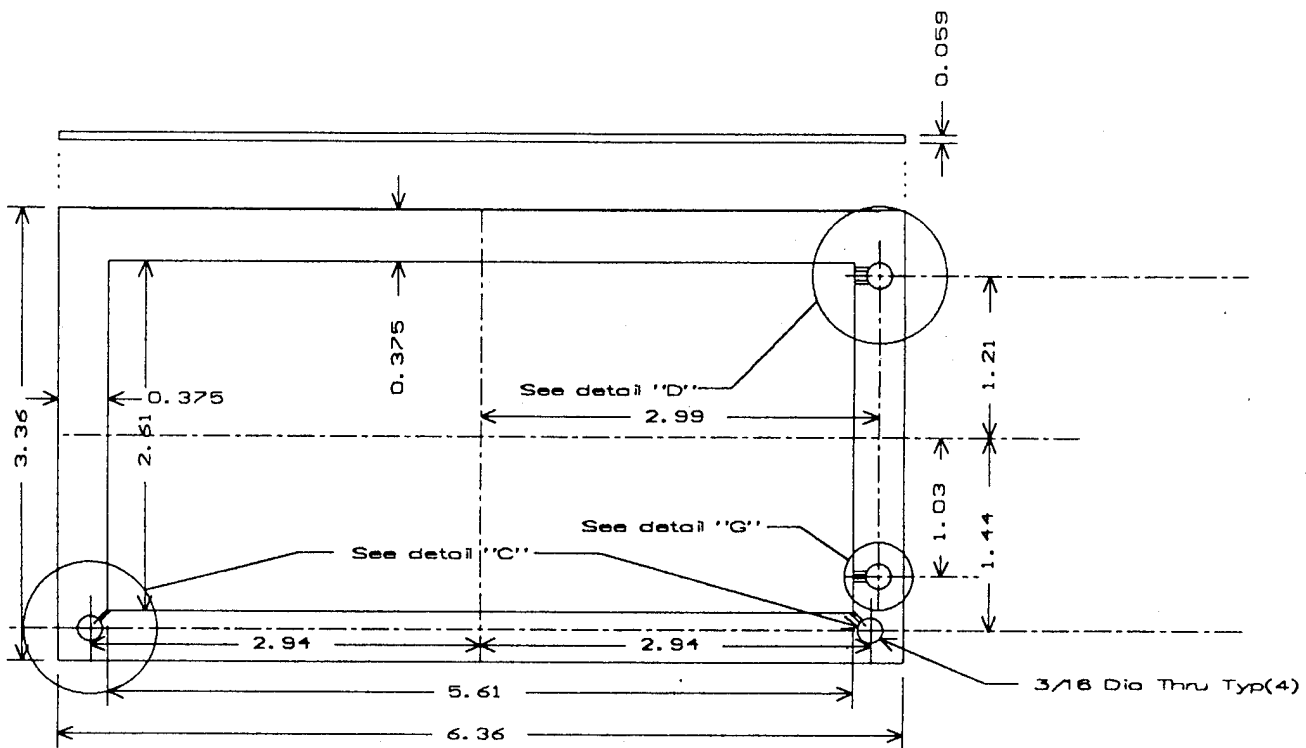


**Figure 16. Polysulfone Anode Frame**

The second piece was an electrically conductive wick, referred to as the hydrophilic anode collector (see **Figure 17**). The hydrophilic anode collector, which was inserted inside the anode frame, was made from a porous carbon paper with channels machined into it. The anode collector was made so that the channels formed a right-to-left labyrinth. The channels of the anode collector allowed eight horizontal passes of hydrogen across the electrode surface of the MEA. Each pass consisted of two parallel channels, 79 mils wide and 40 mils deep, separated by 79 mils. Hydrogen gas, upon leaving the hydrogen entrance manifold through two 26-mil-diameter holes in the upper right-hand corner of the anode frame, entered the anode collector at the upper right-hand corner of the anode collector. The hydrogen gas then flowed to the left through two parallel channels, then the hydrogen turned the corner and flowed to the right through two parallel channels. This flow pattern continues until the hydrogen reaches the lower right-hand corner of the anode compartment. The hydrogen exits the compartment through two 26-mil-diameter holes, which are connected to the hydrogen exit manifold. The bottom rib (marked with repeated "X") is removed from the anode collector. This allows a passage for water

to flow across the bottom of the anode collector. The water entered the anode collector at the lower left-hand corner of the compartment, through one 26-mil-diameter hole in the polysulfone frame. The water flowed across the bottom of the anode collector, just below the level of the hydrogen exit stream, to the lower right-hand corner of the anode compartment. Water flowed from here through one 26-mil-diameter hole in the polysulfone frame to a water-exit manifold, located just below the level of the hydrogen-exit manifold.

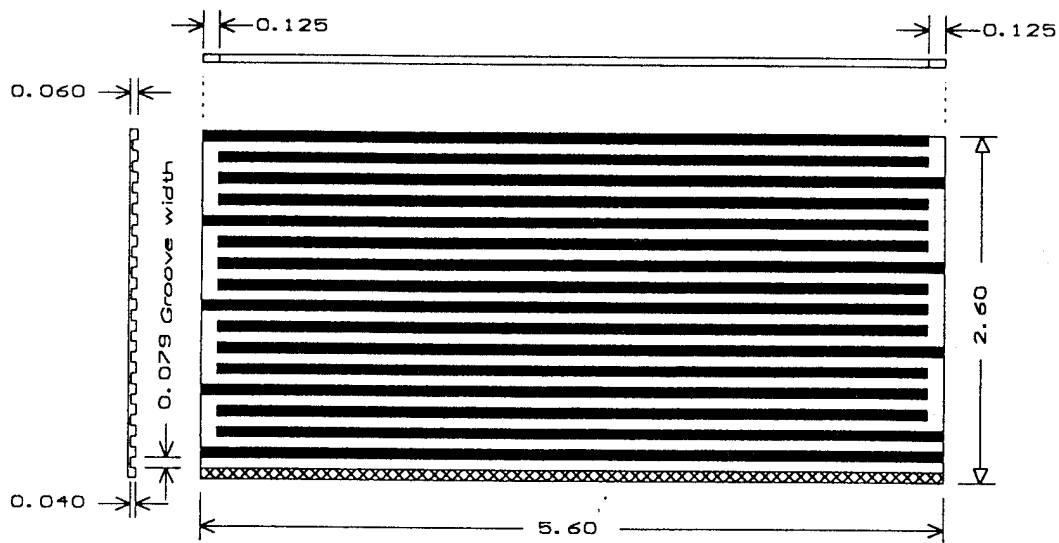


**Figure 17. Hydrophilic Anode Collector**

The cathode compartment design, referred to as a cathode collector, was made from a wet-proofed molded solid carbon plate\* (see **Figure 18**). The flow field consisted of a parallel array of vertical channels. The channels, 125 mils wide and 90-95 mils deep, were separated by 62 mils. Air flowed down through these channels by means of a tangential blower mounted directly above the channels. A combination fine/rough mesh titanium screen package was placed between the MEA and the cathode collector to eliminate water hang-up problems in the cathode air channels. The titanium screen package was enclosed inside a 20-mil polysulfone frame. Additionally, a 25-mil titanium supporting gasket (see **Figure 19**) was placed between the 20-mil polysulfone frame and the cathode collector.

---

\*molded at Giner, Inc.

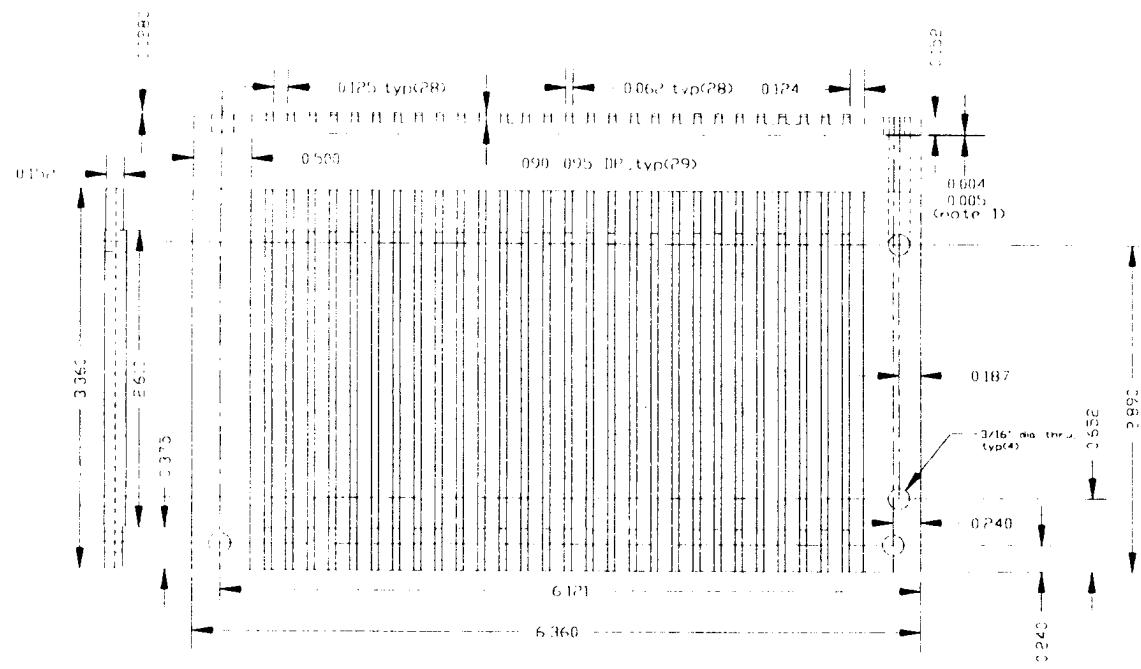


**Figure 18. Cathode Collector**

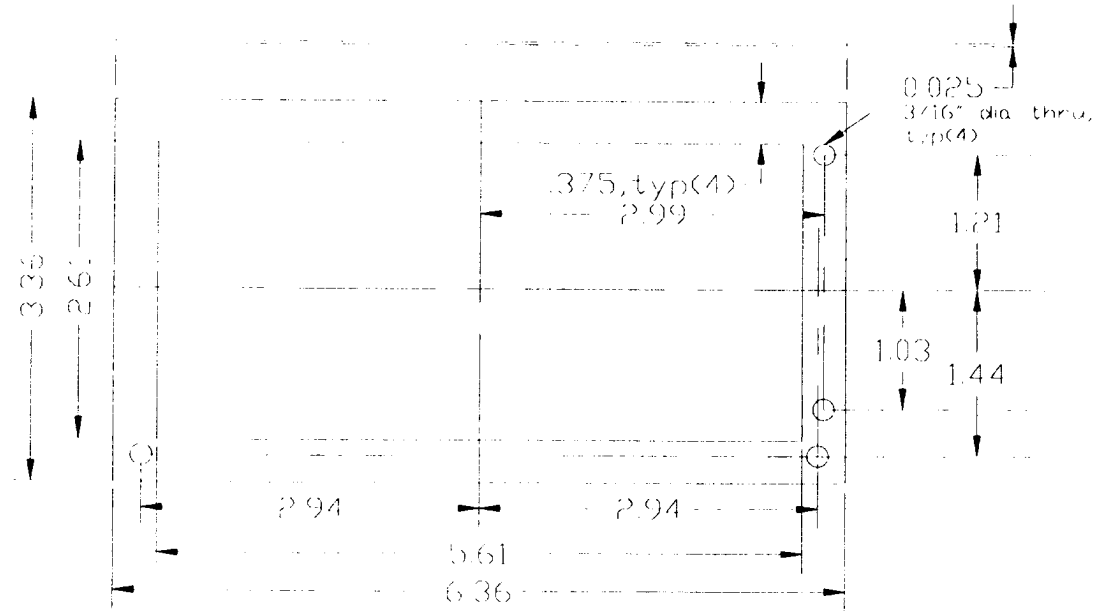


**Figure 19. Titanium Supporting Gasket**

**COPY AVAILABLE TO DTIC DOES NOT PERMIT FULLY LEGIBLE REPRODUCTION**

A platinized niobium sheet was used as a separator sheet between successive cathode and anode compartments. The platinized niobium sheet is referred to as a bipolar separator sheet. Five-mil Teflon sealing gaskets were placed at all surface interfaces. However, 2-3 mil sealing ribs, instead of a standard 5-mil Teflon sealing gasket, were embossed onto the MEA side of the anode frame (the ribs were around the frame perimeter and around the port holes) to provide a sealing surface between the MEA and the anode frame. The MEA (see **Figure 20**) was made of Nafion 120 with two electrode structures (anode and cathode) sharing common centerlines on each side of the membrane, pressed onto both sides of the membrane. The MEA had a 0.1 ft<sup>2</sup> active area.

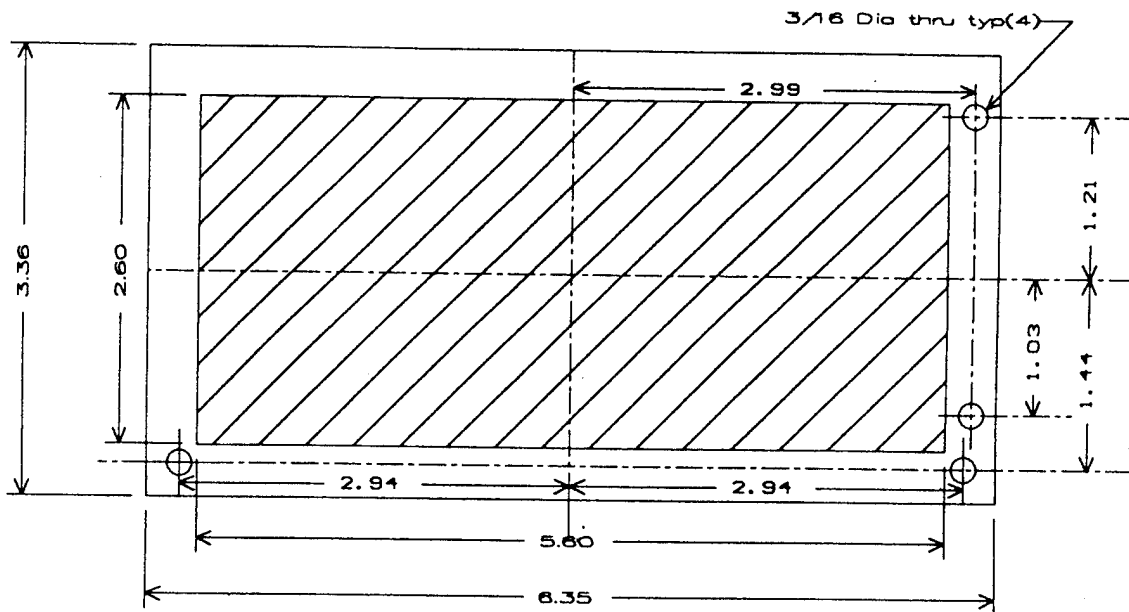


**Figure 20. Membrane and Electrode Assembly**

Figure 1 shows a picture of the baseline stack/system assembled with the titanium end plate system. Figure 2 shows a picture of the baseline stack/system with a pneumatic end plate system. Figures 1 and 2 are located on Page 3 of this report.

The baseline stack/system held in compression by titanium end plates applied a loading of about 1000 psi, while the rubber bladders applied a load of about 200 psi on the 19-cell PEMFC. Both systems operated with bottled H<sub>2</sub> delivered between 10-20 inches (in) H<sub>2</sub>O. This pressure was necessary to overcome the pressure of incoming liquid water. If the H<sub>2</sub>(g) pressure was too low, no H<sub>2</sub>(g) would flow through the system. The H<sub>2</sub>(g) flow rate was monitored by making measurements of the exit H<sub>2</sub>(g) stream with a bubblemeter. Typically the exit H<sub>2</sub>(g) flow rate was 200-400 cc/min at 10-20 inches H<sub>2</sub>O pressure. A large excess of air flow was provided through the cathode air channels.

## 2.4 Results and Discussion

The baseline 19-cell PEMFC stack shown in Figure 1 operated 11.7 V and 117 watts at 100 ASF (see **Figure 21**). The system was running invariantly for approximately 20 minutes and was shut down at the end of the day. Unfortunately, the system performed poorly the next time we started the system, likely due to the presence of excess water in the anode flow fields. The baseline PEMFC stack was subsequently modified by redesigning the anode structure. Additionally, the modified system incorporated the pneumatic end plate system. Hydrogen was delivered to the anode compartments at a higher pressure than usual (about 5 psig). Air flowed through the air channels by convective flow. **Figure 22** shows the performance of the modified system. The stack operated at 13.7 V and 96 watts at 70 ASF.

The present cell design was a departure from the usual. In the interest of simplicity and compactness, the cell was configured such that excess liquid water would be available at the fuel electrode in such a manner as to be attracted to the protons formed in the electrochemical reaction. The protons would electro-osmotically transport liquid water from the fuel side of the membrane to the waste-heat-producing air side, where the temperature would be automatically modulated by the evaporation of the water into the air stream. The concept was, and still is, an exciting one. Since liquid water would be pumped by the protons themselves, the cooling water would flow in proportion to the local current and to the waste heat flux. The higher the current density in a region of membrane, the higher the coolant flow would automatically adjust in the region where it was most needed.

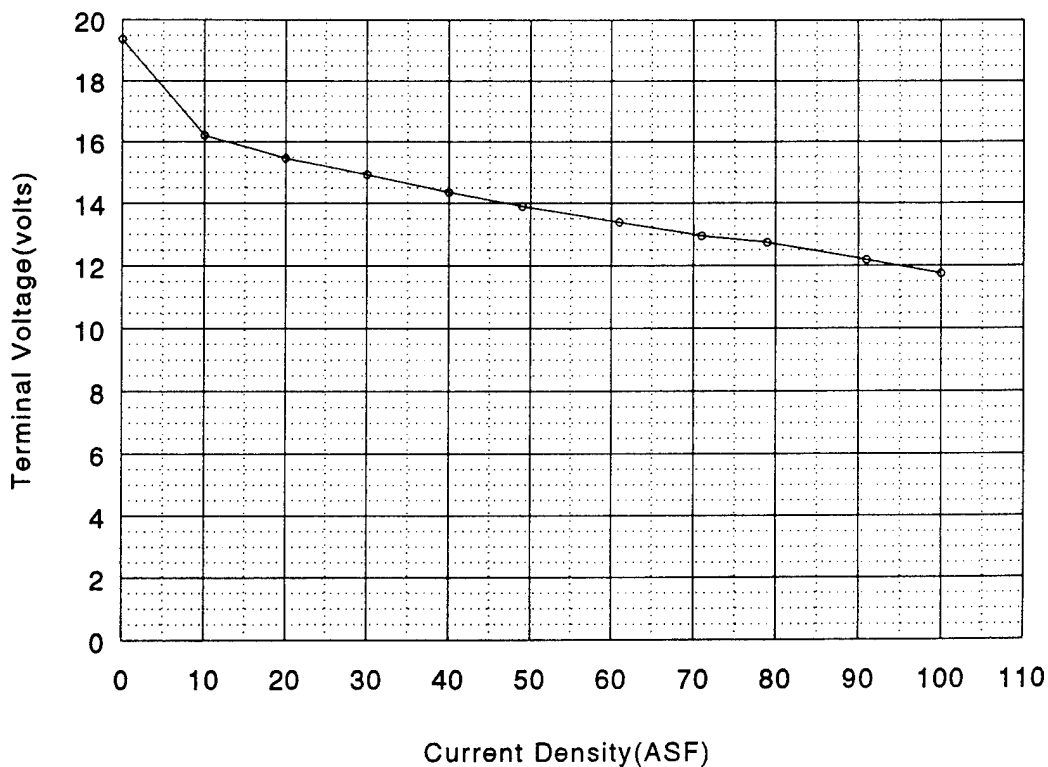


**Figure 21. Performance of H<sub>2</sub>/Air PEM Fuel Cell (9322-1715, 19-Cell Stack)**

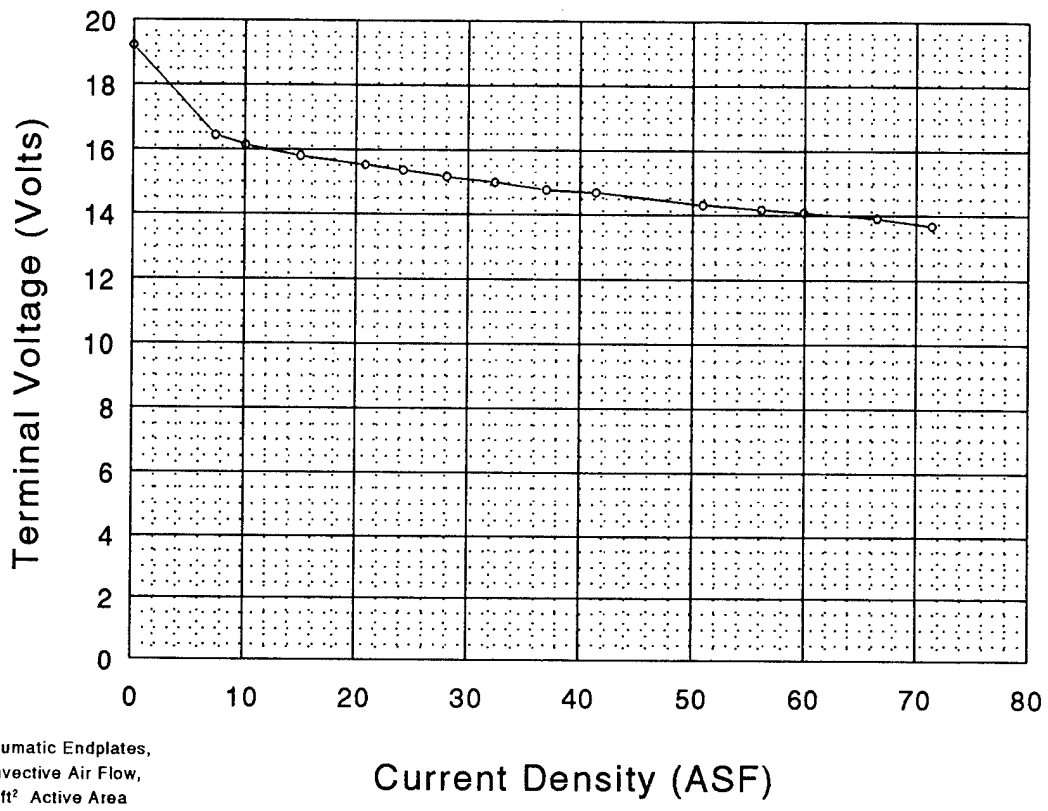


**Figure 22. Performance of H<sub>2</sub>/Air PEM Fuel Cell (19-Cell Stack)**

The means of providing the cooling water was embodied in a hydrophilic current collector which contacted and supplied water to a specially designed anode catalyst. The collector wicked against gravity to avoid flooding the electrode. The development of this unique anode structure resulted in high electro-osmotic water transport from anode to cathode and is considered a significant achievement. The standard MEA design for the baseline fuel cell stack electro-osmotically transported 3 times the product water rate (3.35 cc/hr·cell at 100 ASF) for a total flow rate of about 10 cc H<sub>2</sub>O(l)/hr·cell.

The fuel cell system still requires further development effort. The most notable challenges are incorporating a pneumatic end plate system, without 1) experiencing overboard or manifold leaks at the hydrogen inlet of the anode compartments of the fuel cell and 2) pumping water through the manifold system without "choking" the hydrogen flow to any of the anode compartments. Even so, the results thus far remain encouraging. The 19-cell fuel cell System Design 13 produced just under 120 watts at 100 ASF. We also successfully demonstrated the concept of "proton-water-pumping" to meet the heat-management requirements of a 120-watt fuel cell system.

## **2.5 Conclusions and Recommendations**

The design of the fuel cell stack as it stands is not adequate for long endurance. Short-term results with the fuel cell stack are encouraging (see Figure 21), but the simultaneous drying and flooding of individual fuel cell compartments remain a challenging development concern. The following development areas require further attention.

- (1) Provide a humidification membrane inside the fuel cell system to humidify dry hydrogen before it reaches any anode compartments.
- (2) Develop novel liquid water injection methods that do not lead to flooding or blocking of the anode channels.
- (3) Modify design to reduce thickness of the unitized cathode bipolar plate/air flow field chamber, thus reducing the overall system weight.
- (4) Evaluate stacks containing MEAs fabricated with high-performance membranes (Nafion 117, Nafion 115, Nafion 112) to improve energy density and water back-migration from cathode to anode. Test results during the development phase of the program (**Appendix B, Figure B-3**) indicated that Nafion 117 MEAs show superior performance to Nafion 120.

## Appendix A. Permeability Calculation

$$P_* = \frac{(WDF)(L)}{\Delta P}$$

$$WDF \approx \left( \frac{5 \text{ cc } H_2}{\text{min}} \right) \left( \frac{\text{mole } H_2}{22,400 \text{ cc } H_2} \right) \left( \frac{2 \text{ moles } H_2O}{4 \text{ moles } H_2} \right) = 1.1 \times 10^{-4} \frac{\text{mole } H_2O}{\text{min}}$$

$$\left( \frac{1.1 \times 10^{-4} \text{ mole } H_2O}{\text{min}} \right) \left( \frac{1 \text{ min}}{60 \text{ sec}} \right) \left( \frac{1}{5.08 \text{ cm}^2} \right) = 3.6 \times 10^{-7} \frac{\text{mole } H_2O}{\text{sec } \text{cm}^2}$$

$$P_* = \frac{\left( \frac{3.6 \times 10^{-7} \text{ mole } H_2O}{\text{sec } \text{cm}^2} \right) (5.08 \times 10^{-3} \text{ cm})}{5 \text{ cm Hg}} = 3.66 \times 10^{-10} \frac{\text{mole } H_2O * \text{cm}}{\text{sec} * \text{cm}^2 * \text{cmHg}}$$

$$\left( 3.66 \times 10^{-10} \frac{\text{mole } H_2O * \text{cm}}{\text{sec} * \text{cm}^2 * \text{cmHg}} \right) \left( \frac{22,400 \text{ cc}}{1 \text{ mole } H_2O} \right) = 8.19 \times 10^{-6} \frac{\text{cc } H_2O * \text{cm}}{\text{sec} * \text{cm}^2 * \text{cmHg}}$$

**Appendix B. Summary of System Designs**

## PHASE II: LIGHTWEIGHT PEMFC DEVELOPMENT

### Experimental and Results

Fifteen various fuel cell system configurations were designed, assembled, and tested. The fuel cell systems were comprised of various hardware components. These hardware components can be broken down into various groups; end plates, bipolar separator sheets, anode compartments, cathode compartments, and membrane and electrode assemblies (MEAs). Two end plate designs were used during the Phase II development project. The first design was a standard titanium end plate and the second was a pneumatic end plate system.

The titanium end plates compress the cell components by means of torquing nut and bolt joints, which pass through each end plate. Hydrogen and liquid water enter the fuel cell system from one end and flow towards the other end when using the titanium end plates. Hydrogen enters at the upper left-hand side of the first end plate, then it flows through a manifold toward the second end plate where the hydrogen can then access only the upper left-hand corners of the anode compartment of the fuel cell system. After flowing through a left-to-right labyrinth in the anode compartment the hydrogen exits at the lower left-hand corner of the anode compartments where it flows into the exit manifold, which leaves the fuel cell system at the lower left-hand corner of the first end plate. Liquid water is introduced in the lower right-hand corner of the first end plate just below the level of the hydrogen exit stream. The water flows in a manifold toward the other end plate. The water enters each anode compartment just below the level of the hydrogen exit stream. The water flows horizontally across the anode compartment toward the lower left-hand corner of the anode compartment. The water exits the anode compartment just below the level of the exiting hydrogen stream into another manifold, which exits the fuel cell system at the lower left-hand corner of the first end plate.

The pneumatic end plates compress the individual cell components by means of a rubber bladder inside each end plate. When gas pressure is used to inflate the rubber bladders, spacer plates, also inside each end plate, slide toward each other, thus applying a compression force upon the cell components. The pneumatic end plates employ a fluid feed plate in the center of the system to introduce hydrogen and water to the individual anode compartments. The hydrogen flow enters at the top left-hand corner of the fluid feed plate, splits in half, and simultaneously flows in a manifold toward each pneumatic end plate. The hydrogen enters the anode compartments in the upper left-hand corner, flows from left to right in a labyrinth flow field, and then exits the anode compartment at the lower left-hand corner of the compartment. The hydrogen then flows through a manifold back toward the center of the system where it exits through the fluid-feed plate. Liquid water flows through the lower right-hand corner of the fluid feed plate into a manifold and splits so that water flows toward each end plate. Upon entering each anode compartment, just below the level of the hydrogen exit stream, the water flows horizontally to the lower left-hand corner of the compartment. Water exits each anode compartment into a manifold and flows back toward the center of the system where it will exit through the lower left-hand corner of the fluid feed plate.

The anode compartment included two separate pieces. The first was a polysulfone anode frame with embossed sealing ribs on one side, while the second piece was an electrically conductive wick, referred to as the hydrophilic anode collector (located inside the anode frame), made from a porous carbon paper with channels machined into it. This carbon paper was made such that the resulting flow field was a left-to-right labyrinth. The channels of the anode collector allowed eight passes of hydrogen across the electrode surface of the MEA. Each pass consisted of two parallel channels 79 mils wide and 40 mils deep separated by 79 mils. The bottom rib was removed to allow a gap for liquid water to flow across the bottom of the anode collector.

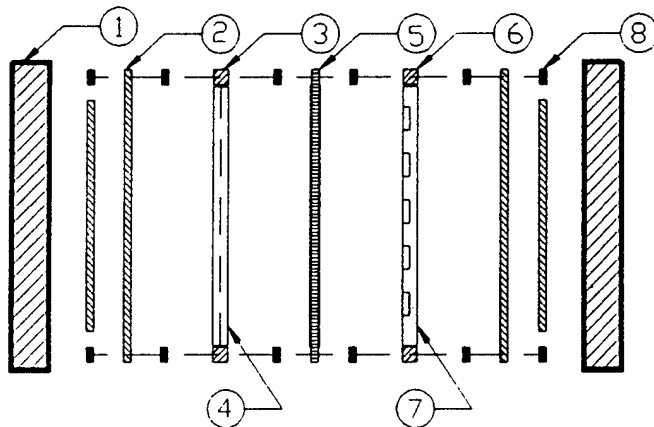
There were two distinct cathode compartment designs. The first design involved a polysulfone cathode frame with machined channels and a porous carbon paper with machined channels positioned inside the cathode frame. This time the carbon paper was made such that the resulting flow field was a parallel array of vertical channels. The second cathode design used a molded solid carbon plate. The flow field consisted of a parallel array of vertical channels. Air flowed through these channels by means of a tangential blower mounted directly above the channels. The MEA, in general, consisted of a membrane (Nafion 120, Nafion 117, or Nafion 105) with two electrode structures (anode and cathode), sharing common centerlines on each side of the membrane, pressed onto both sides of the membrane. All MEAs had an active area of 0.1 ft<sup>2</sup>. Bipolar separator sheets consisted of 3-mil niobium sheets.

The most informative system configurations from the 15 that were evaluated are listed below. A brief description of the configurations and the most significant test results achieved with each is described in the following text.

## System Design 1 - General Description

System Design 1 is a single-cell stack with neither screen packages nor a titanium supporting gasket on the cathode side of the MEA. The cathode side in this design is made of a polysulfone cathode frame with a porous, electrically conductive carbon paper inserted inside the cathode frame. The anode side is made of a polysulfone anode frame with a porous, hydrophilic, electrically conductive carbon paper inserted inside the anode frame. The flow channels in this carbon paper are arranged in a left-to-right labyrinth. The MEA is Nafion 120 with bonded platinum electrode structures. The air channels in the carbon paper are 40 mils deep and 79 mils wide, and they are arranged in a vertical parallel array.

## SYSTEM DESIGN 1



Part number	Part name	Drawing number
1	Endplate	A93-22-145,rev 1
2	Separator	none issued
3	Anode frame	A93-22-130
4	Anode collector	A93-22-131
5	MEA	A93-22-140
6	Cathode frame	A93-22-135
7	Cathode collector	A93-22-138
8	Sealing gasket	A93-22-137

## Results

**Figure B-1** shows typical results for System Design 1. We were able to obtain good performance with oxygen flowing through the cathode channels, (0.81 V at 100 ASF) but air performed poorly (0.66 V at 50 ASF) under the same circumstances. The cathode channels were too small to allow oxygen from air to effectively diffuse through both nitrogen and liquid water film, whereas pure oxygen only had to diffuse through the water film. Additionally, water did not fall from the cathode channels. Water hang-up was a significant problem here. These observations led to System Design 2.

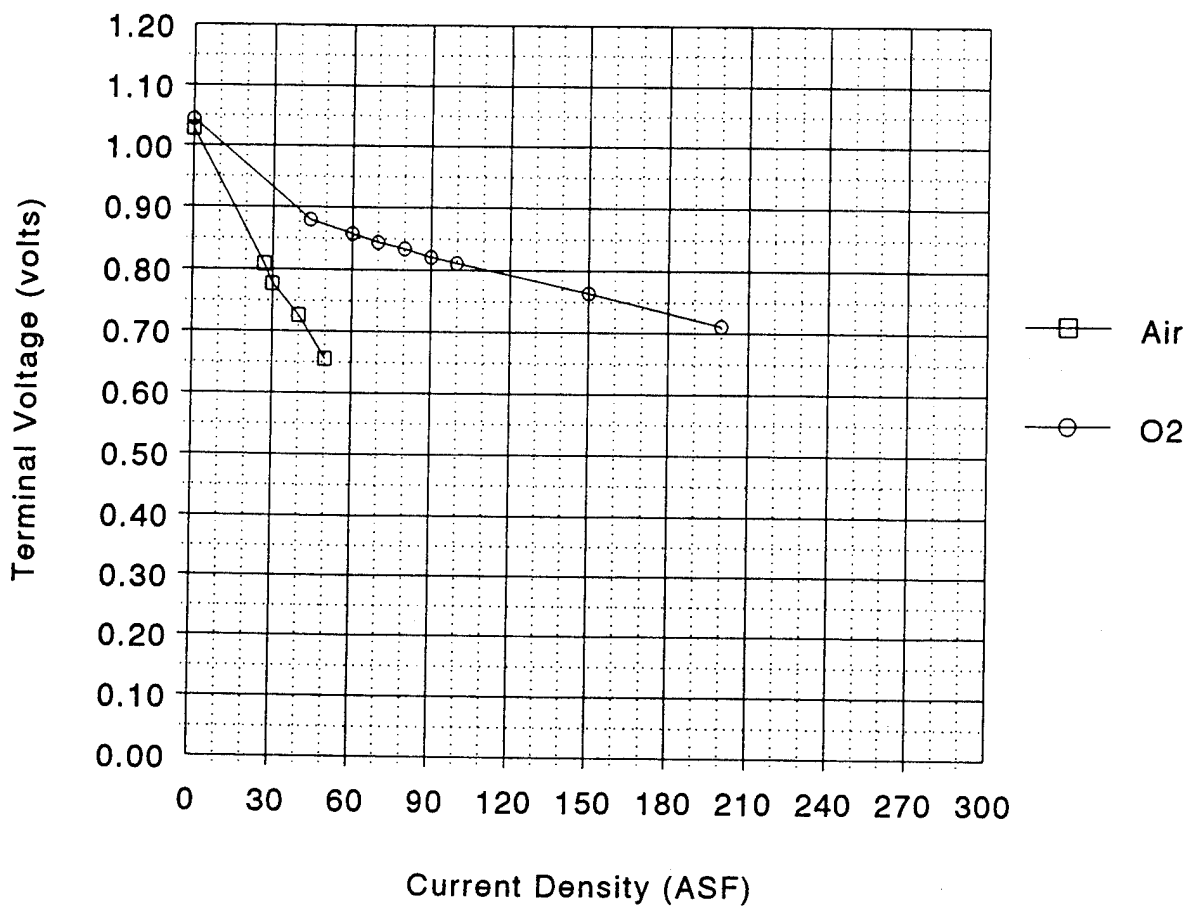
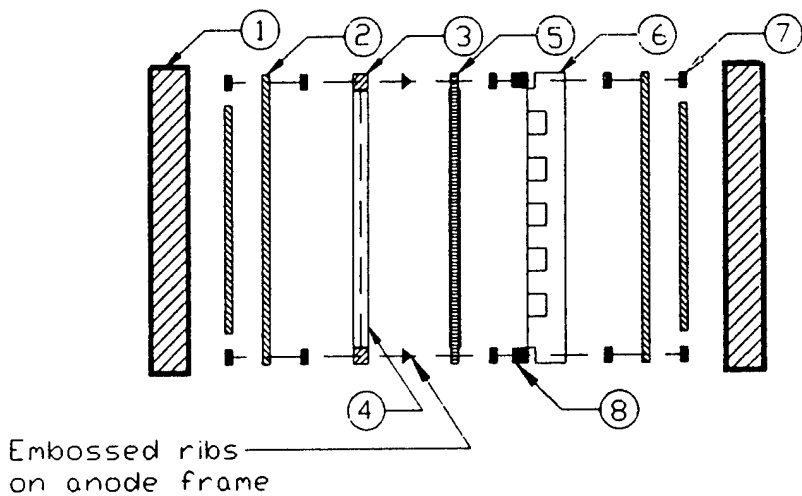


**Figure B-1. H<sub>2</sub>/Air, O<sub>2</sub> PEMFC Performance (Cell #3, 9322-2294)**

## System Design 2 - General Description

System Design 2 is a one-cell stack with no screen packages, but a titanium supporting gasket is included on the cathode side. The anode side of System Design 2 is the same as the anode side of System Design 1, except that we embossed sealing ribs onto the MEA side of the polysulfone anode frame. The cathode side, however, included a solid molded carbon plate with larger flow channels instead of a cathode frame with a porous carbon paper inserted inside. Additionally, the channels on the cathode side are 90-95 mils deep and 125 mils wide.

### SYSTEM DESIGN 2



Part number	Part name	Drawing number
1	Endplate	A93-22-145,rev 1
2	Separator	none issued
3	Anode frame	A93-22-130
4	Anode collector	A93-22-131
5	MEA	A93-22-140
6	Cathode collector	A93-22-135,rev 4
7	Sealing gasket	A93-22-137
8	Supporting gasket	A-93-22-136

### Results

**Figures B-2 and B-3** show that performance with air has dramatically improved in this system (about 0.76 V at 100 ASF). Figure B-2 shows performance with Nafion 120, while Figure B-3 shows performance with Nafion 117. We then proceeded to a three-cell stack.

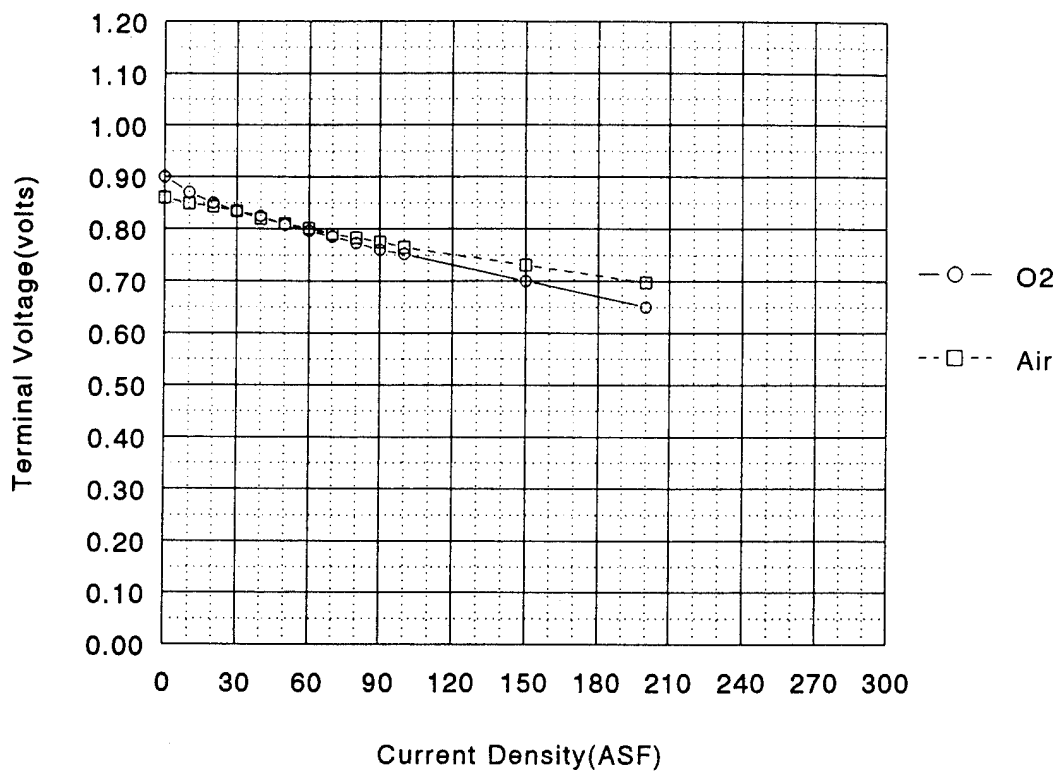
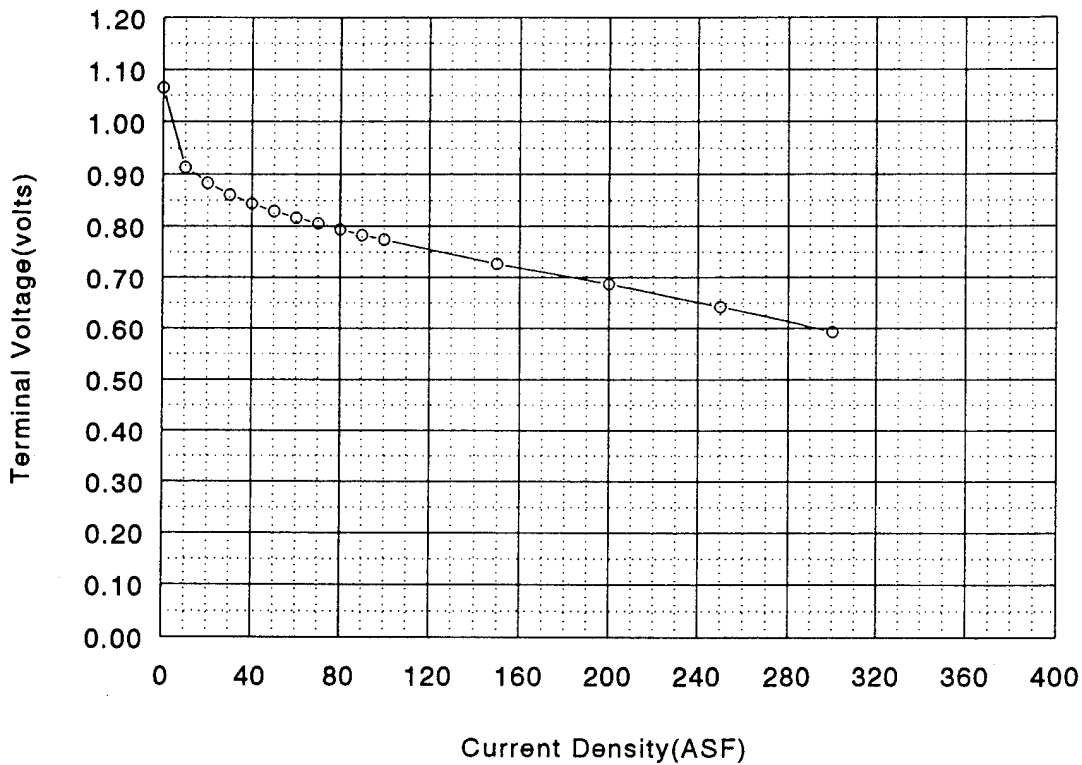


**Figure B-2. H<sub>2</sub>/Air, O<sub>2</sub> PEMFC Performance (Cell #8, 9322-2834)**



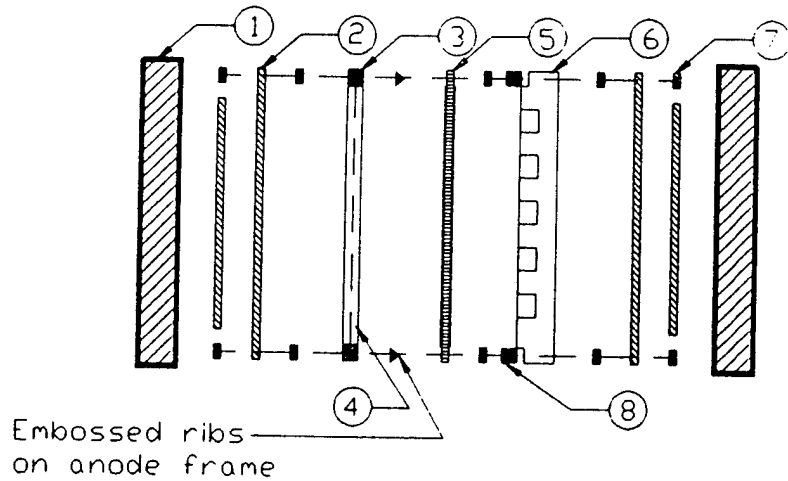
Note: Low pressure H<sub>2</sub> from a bottle and ambient pressure air from a blower

**Figure B-3. Performance of H<sub>2</sub>/Air PEM Fuel Cell (9322-3004, Mea 481-02-1, Nafion 117)**

## System Design 4 - General Description

System Design 4 is a three-cell stack with no screen packages, but the titanium supporting gasket is included on the cathode side. Again the cathode side uses a solid carbon plate. The cathode channels are 90-95 mils deep and 125 mils wide (same hardware as System Design 2).

### SYSTEM DESIGN 4



Part number	Part name	Drawing number
1	Endplate	A93-22-145,rev 1
2	Separator	none issued
3	Anode frame	A93-22-130
4	Anode collector	A93-22-131
5	MEA	A93-22-140
6	Cathode collector	A93-22-135,rev 4
7	Sealing gasket	A93-22-137
8	Supporting gasket	A-93-22-136

## Results

This system operated at 2.2 V at 100 ASF as shown in **Figure B-4**. However, water transport rates (WTR) remain too low (~0.5 - 1.5 x product water rate [PWR]) to maintain the heat management of the final 120-watt system. Therefore, System Design 5, which has the same hardware as System Design 4, is dedicated to increasing the water transport rate. Numerous attempts were made to increase the WTR by making both the anode and cathode structures hydrophilic. We also tried combinations of hydrophilic, hydrophobic electrode structures. We also experimented with different carbon papers that were bonded to the platinum catalyst. A WTR of slightly higher than 2 x PWR was obtained with System Design 5. This was still 1 x PWR short of maintaining the heat management in the final 120-watt system.

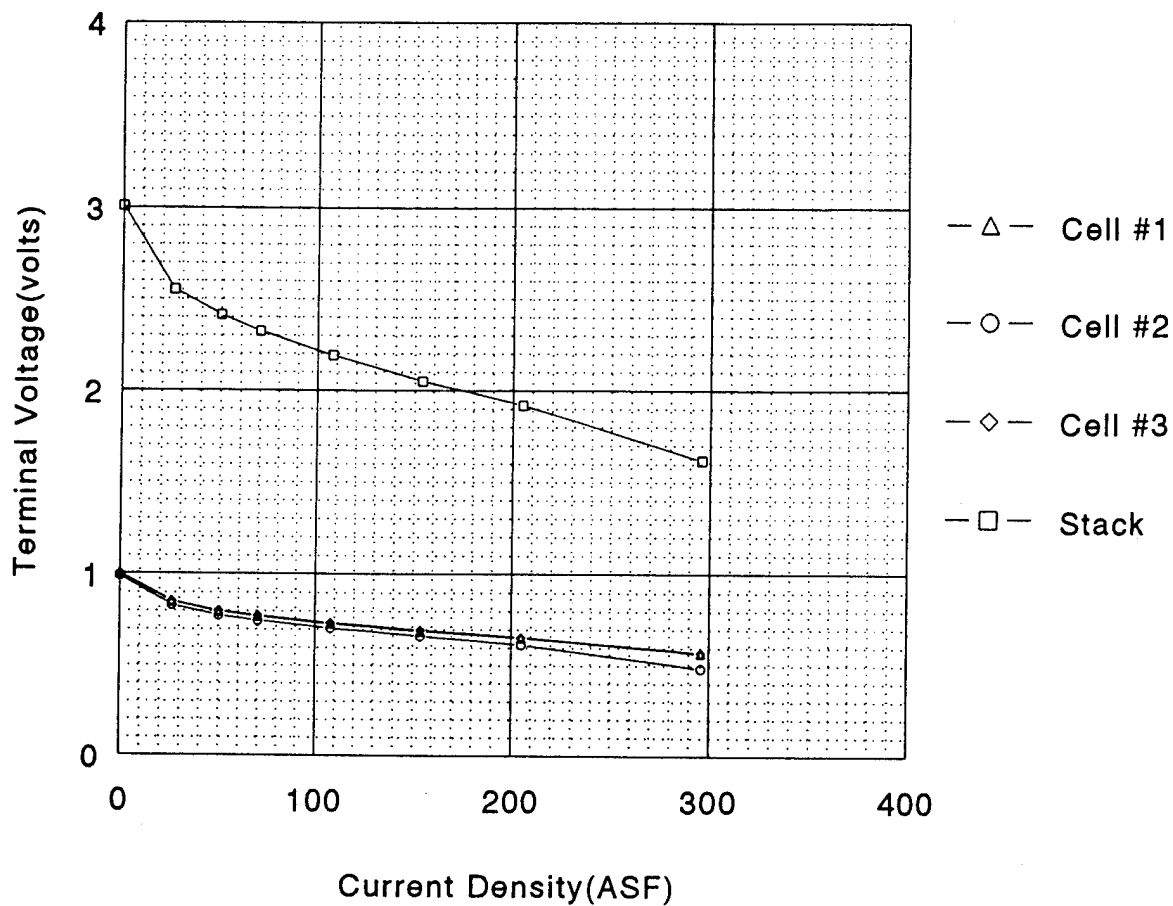
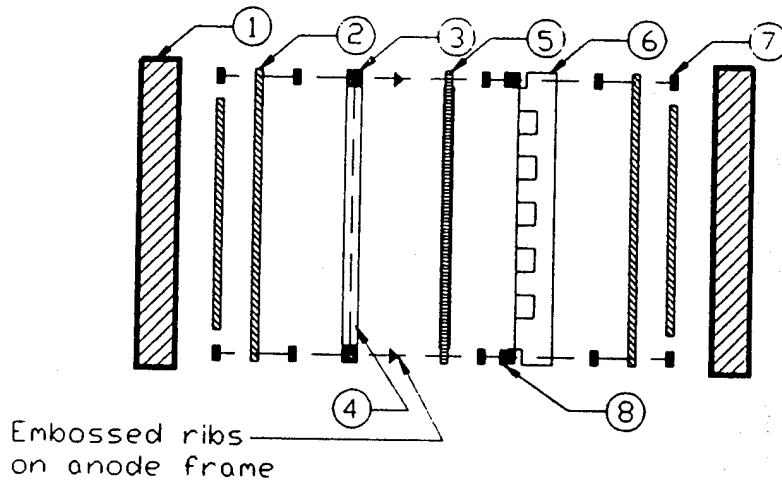


**Figure B-4. Performance of H<sub>2</sub>/Air PEM Fuel Cell (9322-3084, 3-Cell Stack)**

## System Design 6 - General Description

System Design 6 is a five-cell stack with no screen packages. The hardware is the same as System Design 4.

### SYSTEM DESIGN 6



Part number	Part name	Drawing number
1	Endplate	A93-22-145,rev 1
2	Separator	none issued
3	Anode frame	A93-22-130
4	Anode collector	A93-22-131
5	MEA	A93-22-140
6	Cathode collector	A93-22-135,rev 4
7	Sealing gasket	A93-22-137
8	Supporting gasket	A-93-22-136

## Results

System Design 6 operated at 3.5 V at 100 ASF (see **Figure B-5**). This is an encouraging result; however, the water transport rates still remain low. We worked on the water transport rates in System Design 7 and System Design 8. We found that a Nafion 120 MEA with an exposed platinum catalyst layer on the anode side improved the WTR to 3 x PWR, while still delivering good performance at 100 ASF. This MEA design uses Nafion 120 with platinum catalyst electrodes on both sides of the membrane. A WTR of 3 x PWR was achieved which should meet the heat management requirements of the final 120-watt system. However, we experienced water hang-up problems in the cathode channels were experienced.

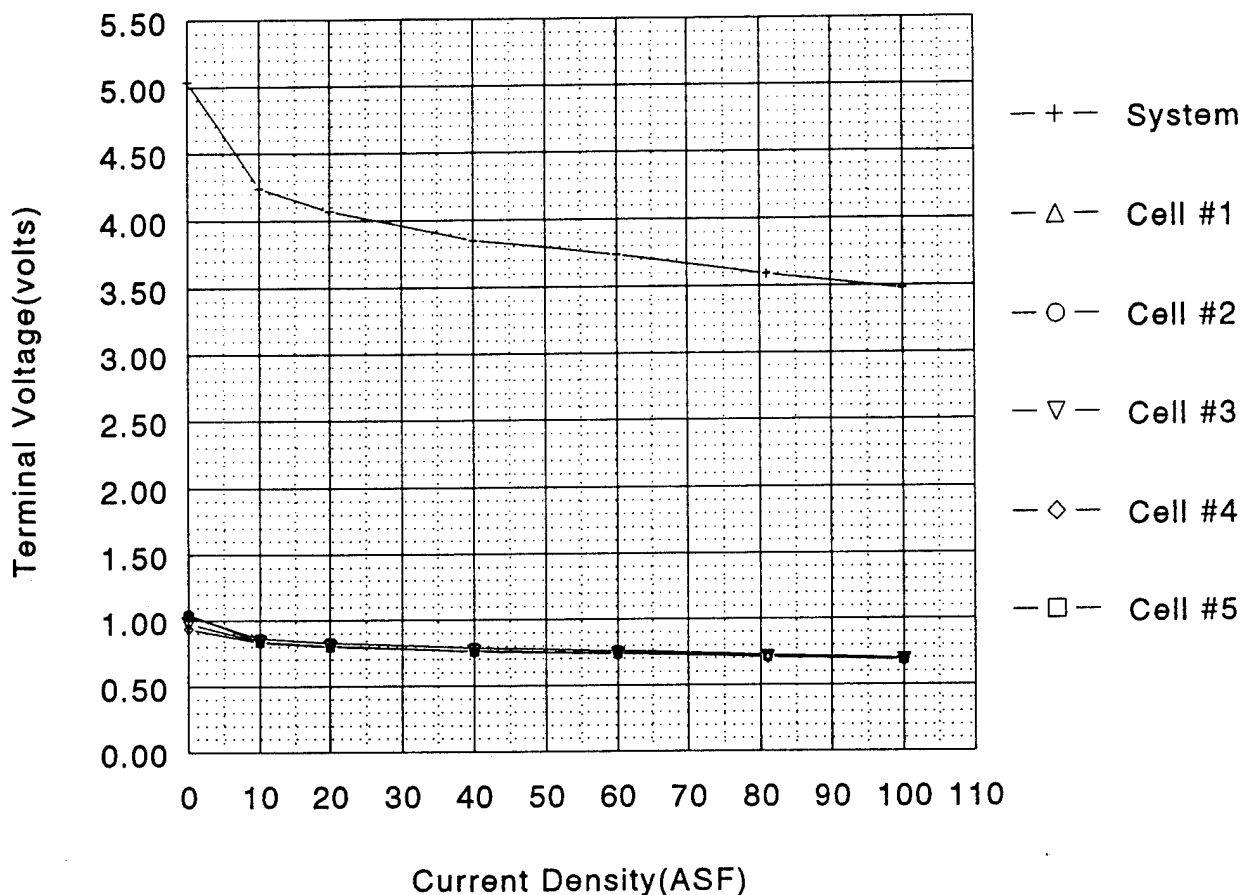
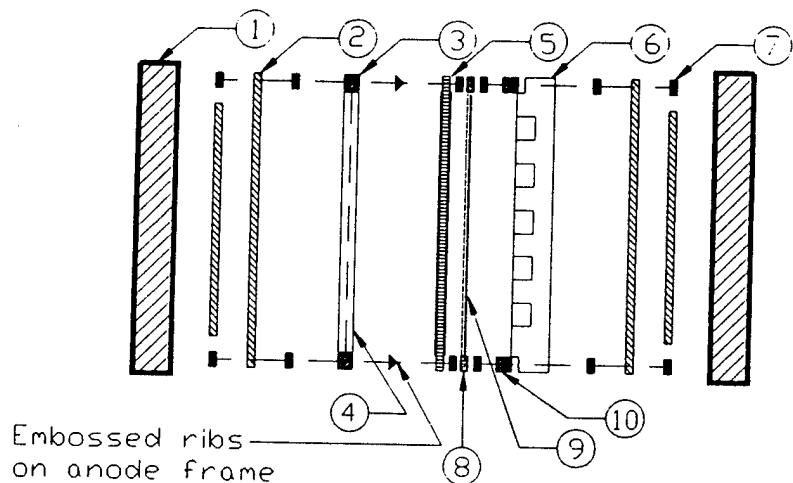


**Figure B-5. Performance of H<sub>2</sub>/Air PEM Fuel Cell (9322-0195, 5-Cell Stack)**

## System Design 9 - General Description

System Design 9 is a one-cell stack with the same hardware as System Design 6, except that we have added a screen package consisting of a fine and a rough mesh titanium screen.

### SYSTEM DESIGN 9



Part number	Part name	Drawing number
1	Endplate	A93-22-145,rev 1
2	Separator	none issued
3	Anode frame	A93-22-130
4	Anode collector	A93-22-131
5	MEA	A93-22-140
6	Cathode collector	A93-22-135,rev 4
7	Sealing gasket	A93-22-137
8	Polysulfone shim	none issued
9	Ti screen package	none issued
10	Supporting gasket	A-93-22-136

### Results

This system design resolved the water hang-up problem in the cathode channels. This system operated at 0.67 V at 100 ASF (see **Figure B-6**). We proceeded to scale this system up to a five-cell stack.

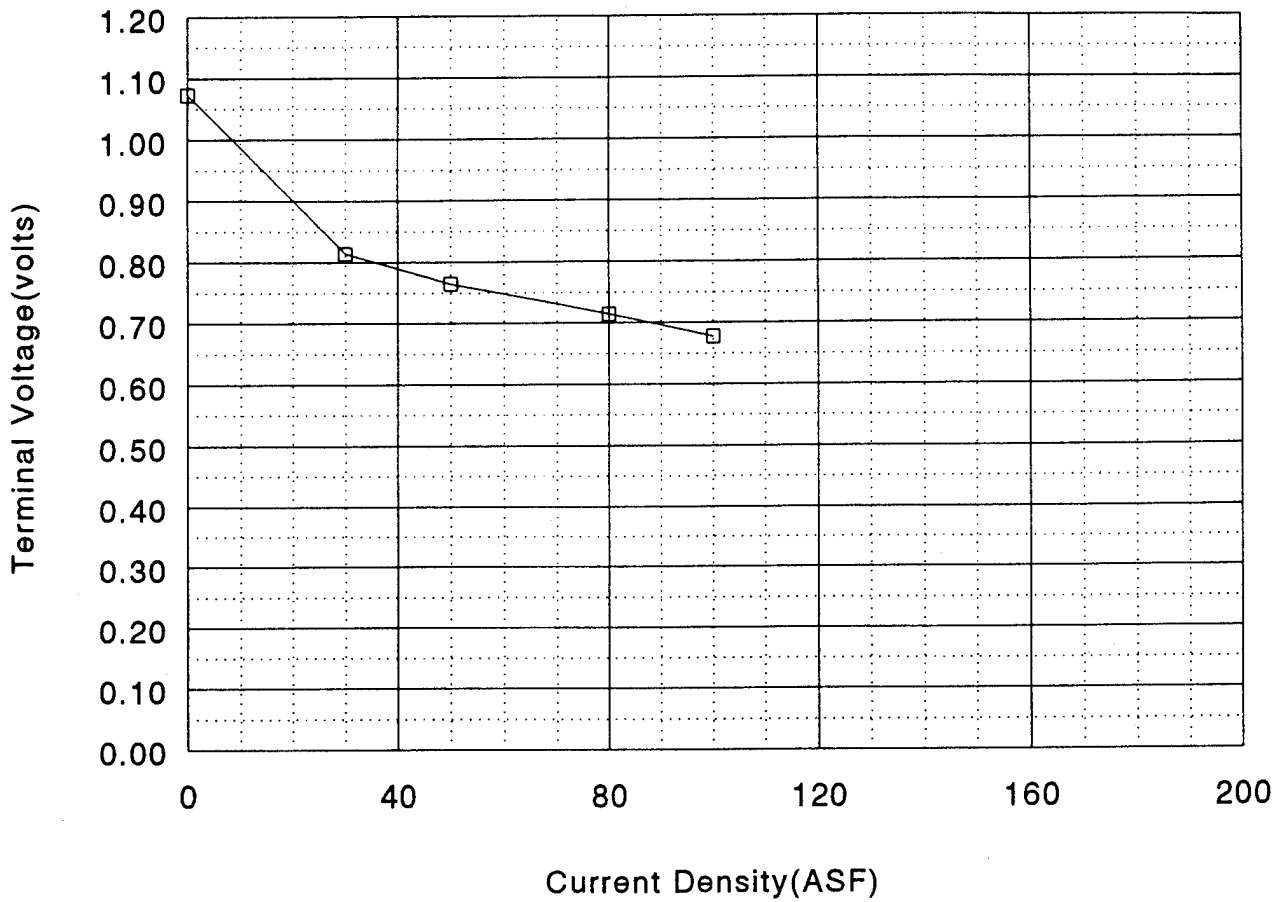
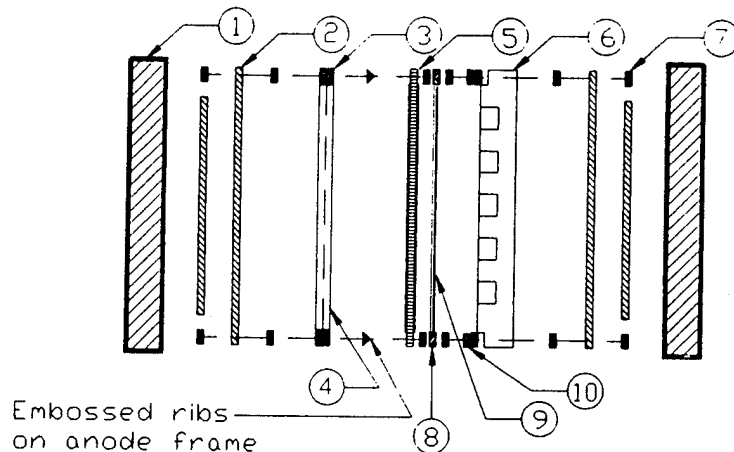


**Figure B-6. Performance of H<sub>2</sub>/Air PEM Fuel Cell (9322-0655)**

## System Design 10 - General Description

System Design 10 is a five-cell stack with the same configuration as System Design 9.

### SYSTEM DESIGN 10



Part number	Part name	Drawing number
1	Endplate	A93-22-145,rev 1
2	Separator	none issued
3	Anode frame	A93-22-130
4	Anode collector	A93-22-131
5	MEA	A93-22-140
6	Cathode collector	A93-22-135,rev 4
7	Sealing gasket	A93-22-137
8	Polysulfone shim	none issued
9	Ti screen package	none issued
10	Supporting gasket	A-93-22-136

### Results

This system operated at 3.3 V at 100 ASF (see **Figure B-7**) for 4.5 hours. The wicks/current collectors on the anode side subsequently started to dry out. We also encountered a cross-membrane hole located at the H<sub>2</sub> (g) inlet port of Cell #2.

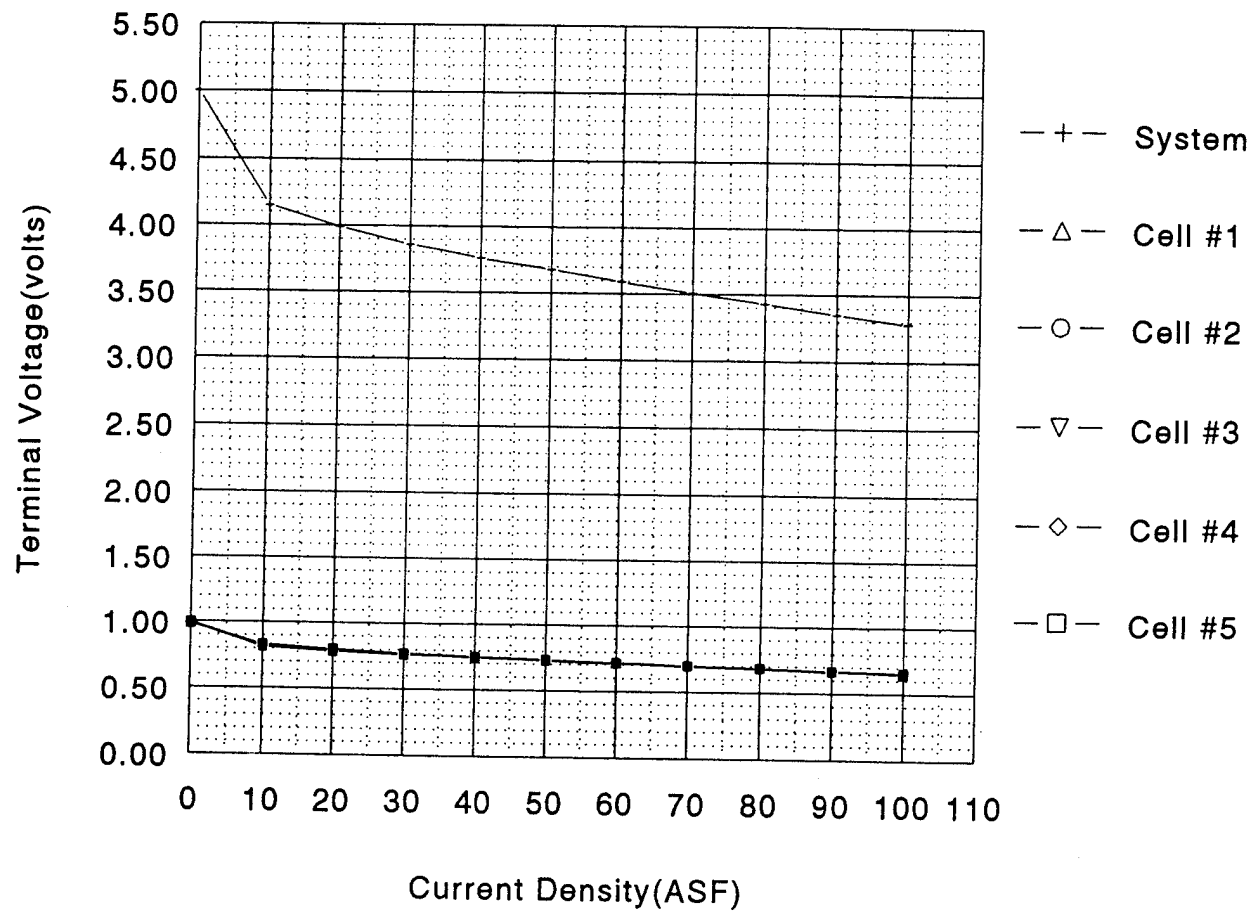
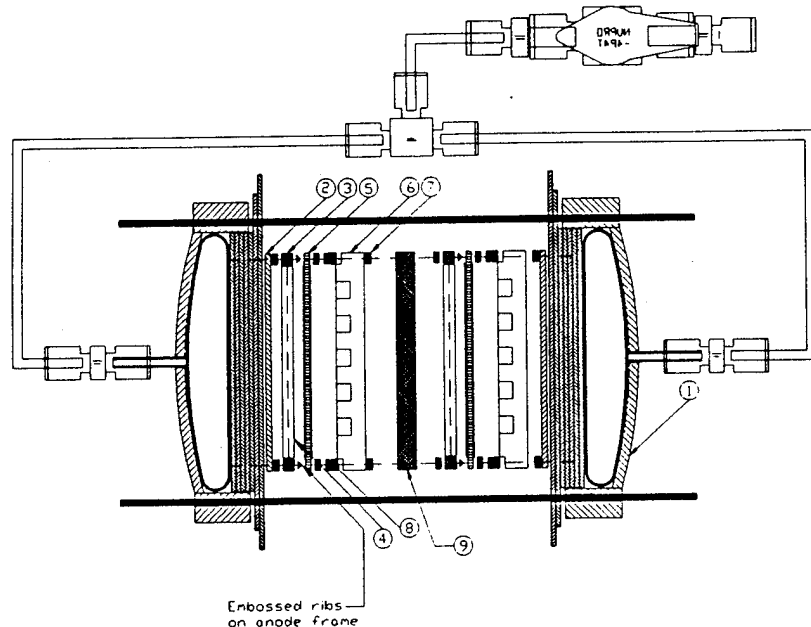


**Figure B-7. Performance of H<sub>2</sub>/Air PEM Fuel Cell (9322-0695, 5-Cell Stack)**

## System Design 11 - General Description

System Design 11 is a 19-cell stack with pneumatic end plates. The hardware is the same as System Design 10, except there are no screen packages. Additionally, a fluid feed plate is located in the center of the stack where hydrogen and water will enter and leave the system.

### SYSTEM DESIGN 11



Part number	Part name	Drawing number
1	Pneumatic endplate	9322-300-000
2	Separator	none issued
3	Anode frame	A93-22-130
4	Anode collector	A93-22-131
5	MEA	A93-22-140
6	Cathode collector	A93-22-135,rev 4
7	Sealing gasket	A93-22-137
8	Supporting gasket	A-93-22-136
9	Fluid feed plate	9322-301

### Results

System Design 11 operated at 11.5 V at 50 ASF (see Figure B-8) for a very short period of time. We encountered considerable overboard leaks. We also observed a cross-membrane hole located at the H<sub>2</sub> (g) inlet port of Cell #17.

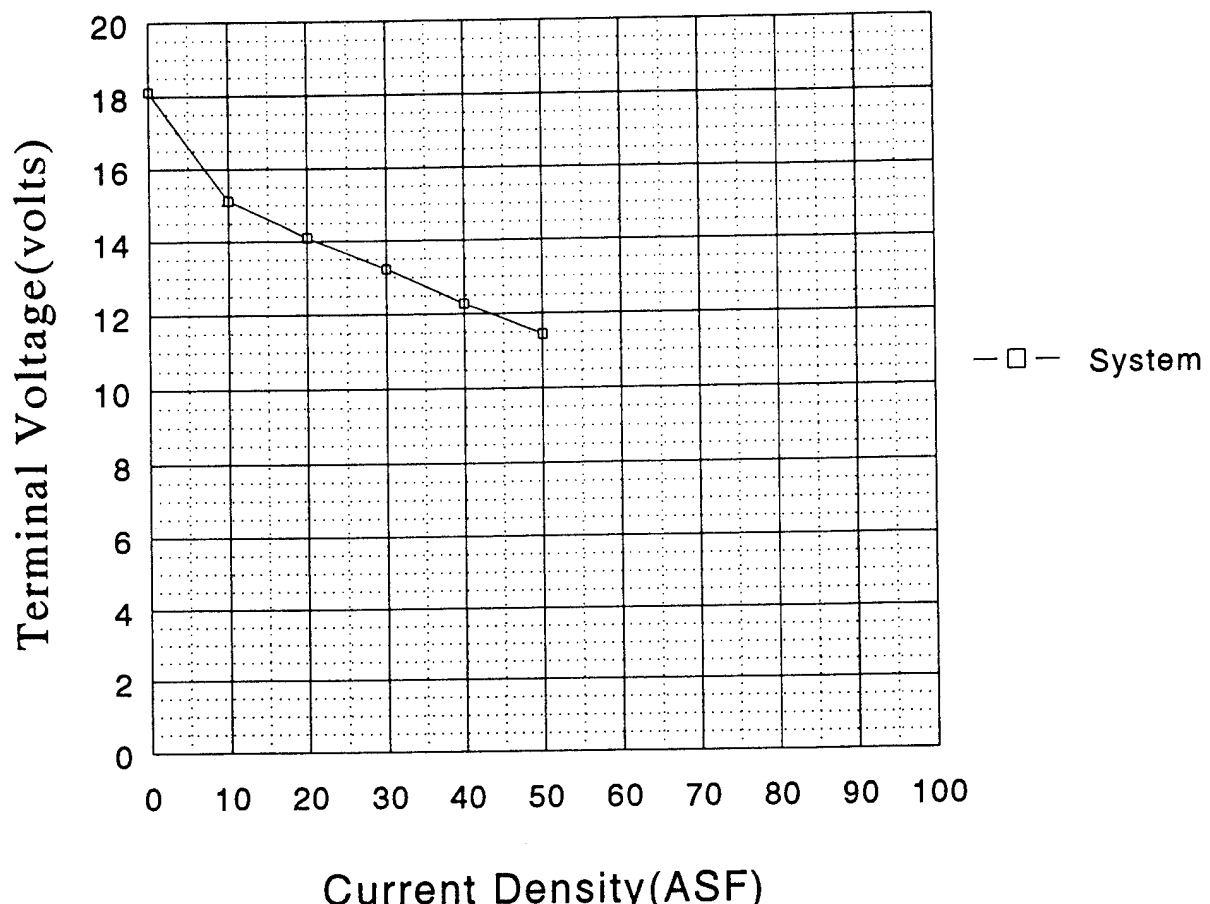
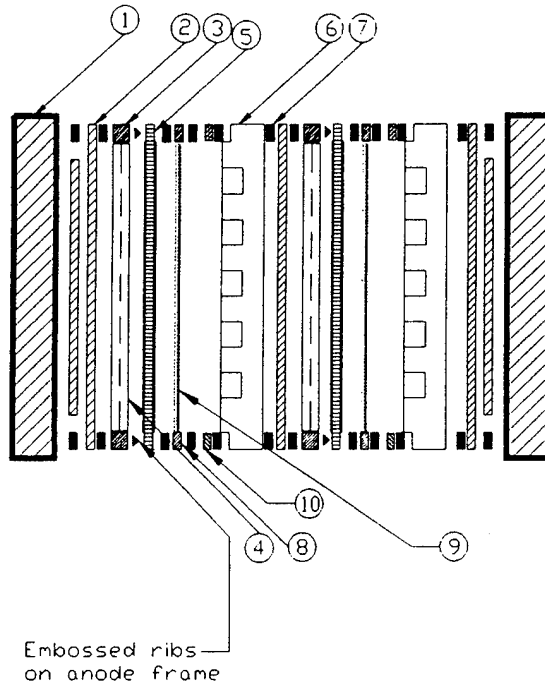


Figure B-8. Performance of H<sub>2</sub>/Air PEM Fuel Cell (9322-1435, 19-Cell Stack)

## System Design 13 - General Description

System Design 13 is a 19-cell stack (same as System Design 11) except this system includes the fine/rough mesh titanium screen package from System Design 9. We also used titanium end plates instead of pneumatic end plates, therefore, there was no need for a fluid feed plate in the center of the system.

## SYSTEM DESIGN 13



Part number	Part name	Drawing number
1	Endplate	A93-22-145,rev 1
2	Separator	none issued
3	Anode frame	A93-22-130
4	Anode collector	A93-22-131
5	MEA	A93-22-140
6	Cathode collector	A93-22-135,rev 4
7	Sealing gasket	A93-22-137
8	Polysulfone shim	none issued
9	Ti screen package	none issued
10	Supporting gasket	A-93-22-136

## Results

This system operated 11.7 V at 100 ASF (see **Figure B-9**) for 20 minutes. The system was running very well, but was shut down at the end of the day. Unfortunately, the system performed poorly the next time we started the system.

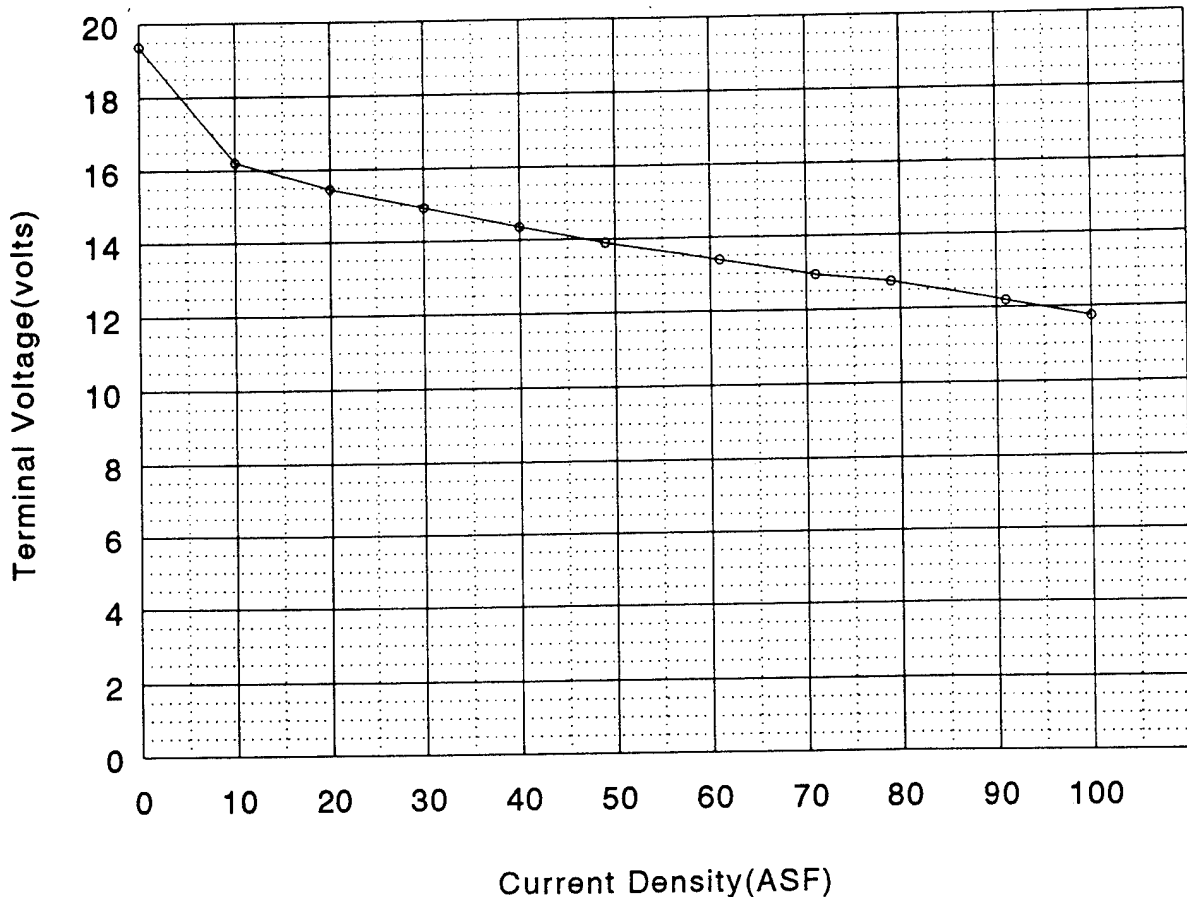


**Figure B-9. Performance of H<sub>2</sub>/Air PEM Fuel Cell (9322-1715, 19-Cell Stack)**

#### **System Designs 14 and 15 - General Description**

System Design 14 and 15 have the same configuration as System Design 13. We attempted to solve the simultaneous flooding and drying problems that are occurring throughout the stack.

#### **Results**

We have been unsuccessful to date. Cells at the end of the stack continue to dry out. Any attempt to increase water flow only drops the performance of the stack due to flooding of other cells. At best, the system operated at 13-14 V at 50 ASF for 2.5 hours.